GEO Newsletter

Group for Earth Observation

Group for Earth Observation

No 80 - December 2023

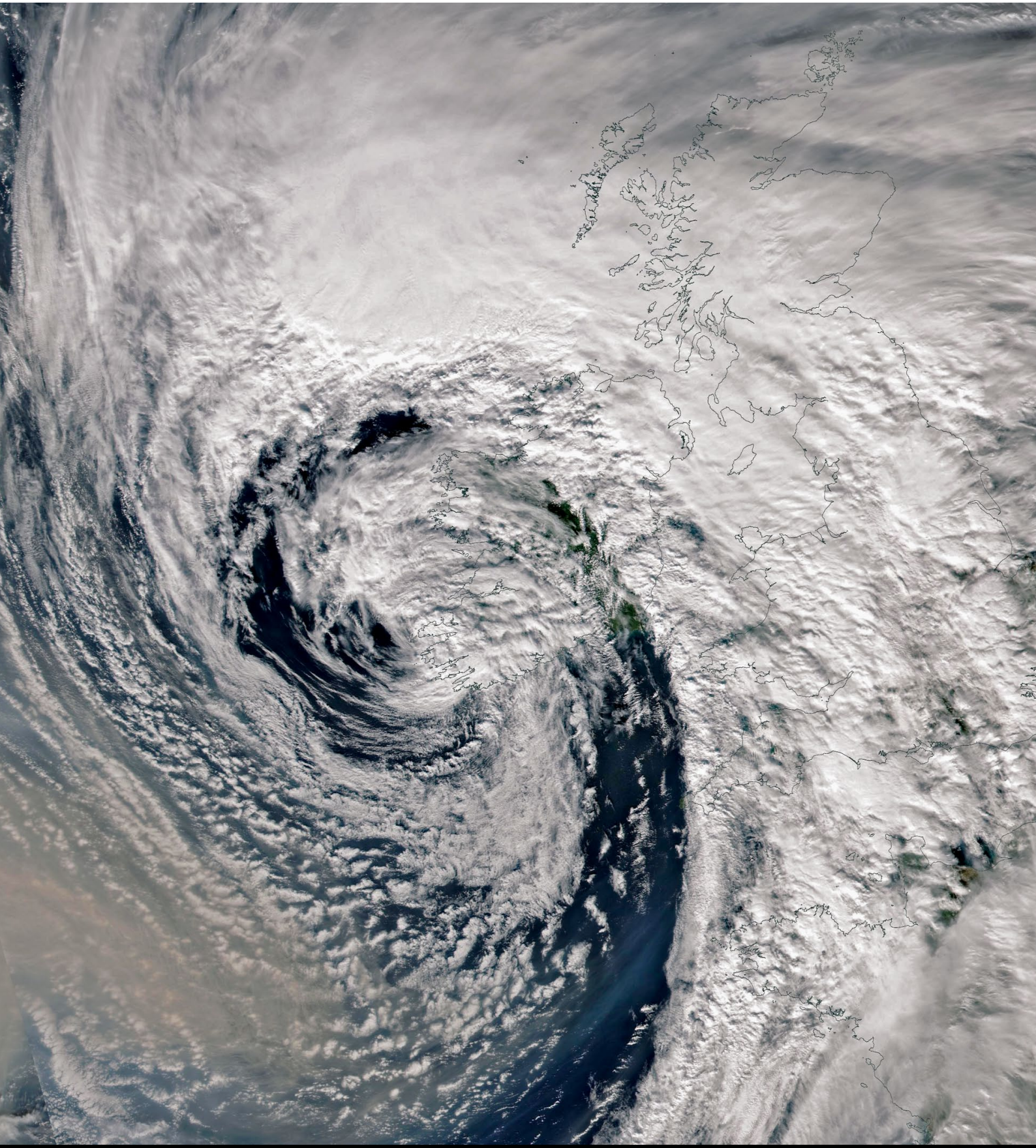

Agnes, the first named storm of the season, is, pictured in this NOAA 20 image from September 27, 2023 over the British Isles, where it brought sustained heavy rainfall and winds exceeding 100 kilometres per hour

Image: NASA Worldview Snapshots

Copy for the Newsletter

The Editor is always delighted to receive material for inclusion in the GEO Quarterly Newsletter. These can relate to any aspect of Earth Imaging, especially

- Technical articles concerning relevant hardware and software
- Construction projects
- Weather satellite images
- Reports on weather phenomena
- Descriptions of readers' satellite imaging stations
- Activities from overseas readers
- Letters to the Editor
- Problems and Queries for our experts to answer

Contributions should of course be original and be submitted to the editor by e-mail not later than the middle of the month preceding publication.

If your article submission contains embedded images and diagrams, please note that you must also submit copies of the original images as separate attachments: these are essential for page make-up purposes.

Materials for publication should be sent to the editor, Les Hamilton, at

geoeditor@geo-web.org.uk

Useful User Groups

Weather Satellite Reports

This group provided weekly reports, updates and news on the operational aspects of weather satellites.

https://groups.io/g/weather-satellite-reports

SatSignal

This end-user self help group is for users of David Taylor's Satellite Software Tools, including the orbit predictor WXtrack, the file decoders GeoSatSignal and SatSignal, the HRPT Reader program, the remapper GroundMap, and the manager programs - MSG Data Manager, GOES-ABI Manager, AVHRR Manager etc.

https://groups.io/g/SatSignal

MSG-1

This forum provides a dedicated area for sharing information about hardware and software for receiving and processing EUMETCast data.

https://groups.io/g/MSG-1

GEO-Subscribers

This is the official group is for subscribers of the Group for Earth Observation (GEO), aimed at enthusiasts wishing to exchange information relating to either GEO or Earth Observation satellites.

https://groups.io/g/GEO-Subscribers/

Visit GEO on Facebook

http://www.facebook.com/groupforearthobservation

GEO
Group for Earth Observation

and follow the dozens of links to NOAA, NASA, ESA, EUMETSAT and much more ...

From the Editor

Les Hamilton

The front cover of this issue carries the somewhat beautiful and beguiling image of Agnes, the first named storm to hit western Europe, the start of an unprecedented spell of high winds, rain and widespread flooding. With four such events already, let's hope that the weather follows a much smoother path through December and into the New Year.

If the Meteor M 2-3 satellite launched during the summer has proved to be less than overwhelming in its performance, it is to be hoped that its successor, Meteor M 2-4, which is now provisionally due to launch in the early hours of February 22, 2024 from the Vostochny, Cosmodrome, will prove to be the real deal. In the meantime, the article on page 16 describes how to make the best of this satellite's below par infrared channel.

Looking forward to next year, it would be great if more readers provided articles sharing their experiences in the field of satellite imaging. In this issue, Richard continues his treatise on visualising the derived products provided on EUMETCast.

To all our readers, we wish you a pleasant Festive Season and a Happy New Year.

Contents

The Biesbosch of the Netherlands

NASA Earth Observatory

Story by Lindsey Doermann

NASA Earth Observatory image by Lauren Dauphin, using Landsat data from the U.S. Geological Survey

Within the Netherlands' De Biesbosch National Park, abundant wildlife—from beavers and otters to kingfishers and egrets—thrive among reed beds and willow stands. But the verdant appearance of this large freshwater tidal wetland belies what is really a highly engineered landscape. The defining event shaping it today was a devastating flood in the 15th century. Since then, it has continued to evolve under the forces of rivers, tides, and human efforts to manage the water.

This image shows the national park, which was established in 1994, within the lower Rhine and Meuse delta. Agricultural land and the industrial port city of Dordrecht, which flank the wetlands, are also visible. The image was acquired by the OLI (Operational Land Imager) on Landsat 8, on July 8, 2023.

In November 1421, an extratropical cyclone struck the region, setting off what is known historically as St. Elizabeth's flood. Swollen rivers and tidal surges led to dyke failures. The floodwaters destroyed numerous villages and probably claimed thousands of victims in the area that is now the Biesbosch.

That flood created a large inland sea, where, over time, rivers and tides deposited sediments, and the landscape gradually morphed into one of islands and winding waterways. Reeds and grass-like aquatic plants called rushes established themselves on the sandy banks (Biesbosch roughly translates to "forest of rushes"), and some of the land was reclaimed for agriculture.

In recent centuries, a series of major engineering projects helped to transform the Biesbosch into a largely human-dominated landscape. Prominent in the image are the Nieuwe Merwede canal, built in the mid-19th century for flood control, and three reservoirs including De Gijster, constructed in the 1970s to store water for domestic and industrial uses.

But instances of flooding persisted into the 20th century, including a deadly and damaging flood in 1953. Following that event, the Dutch Ministry of Infrastructure and Water Management embarked upon a massive flood control project called the Delta Works. The initiative included building new sluices to close off the Haringvliet estuary, a North Sea inlet downstream of the Biesbosch. When this

continued at the foot of page 5

Spectacular Sediment in Van Diemen Gulf

MODIS Web Image of the Day

The colorful waters of Van Dieman Gulf sit off the Northern Territory of Australia, partially surrounded by the Cobourg Peninsula and Melville Island. The landscape of Northern Territory is characterized by open, sparsely populated lands with higher elevations in the north and a relatively flat, arid, and red-soil-filled coastal region. As rivers flow from higher elevations toward Van Diemen Gulf, they pick up reddish-tan sediment which is ultimately deposited in in the blue waters offshore. This sediment, along with tidal motion in the shallow gulf, creates stunning patterns that almost appear to glow when viewed from space.

The Moderate Resolution Imaging Spectroradiometer (MODIS) on board NASA's Aqua satellite acquired a true-color image of Van Diemen Gulf of September 22, 2023.

NASA's Aqua satellite captured this 250 metre resolution image of Australia's Van Diemen Gulf on September 23, 2023.
Image Credit: MODIS Land Rapid Response Team, NASA GSFC

The Biesbosch

continued from previous page

was completed in 1970, tidal ranges in the Biesbosch dropped from approximately 1.9 metres to around 0.4 metres.

Today, visitors to the national park explore the flora and fauna of the protected natural area via hiking trails and waterways. The ecosystem they experience evolves, as well. For example, a rewilding organisation is investigating whether the waterways can again support European sea sturgeon (Acipenser sturio). This anadromous fish was once abundant in the Rhine delta but has not been seen in Dutch waters for decades due to overfishing, degraded water quality, and obstructed channels. Dozens of young sturgeon were recently released into the Biesbosch to determine if a larger reintroduction might be successful.

Western Canada Engulfed in Smoke

MODIS Web Image of the day

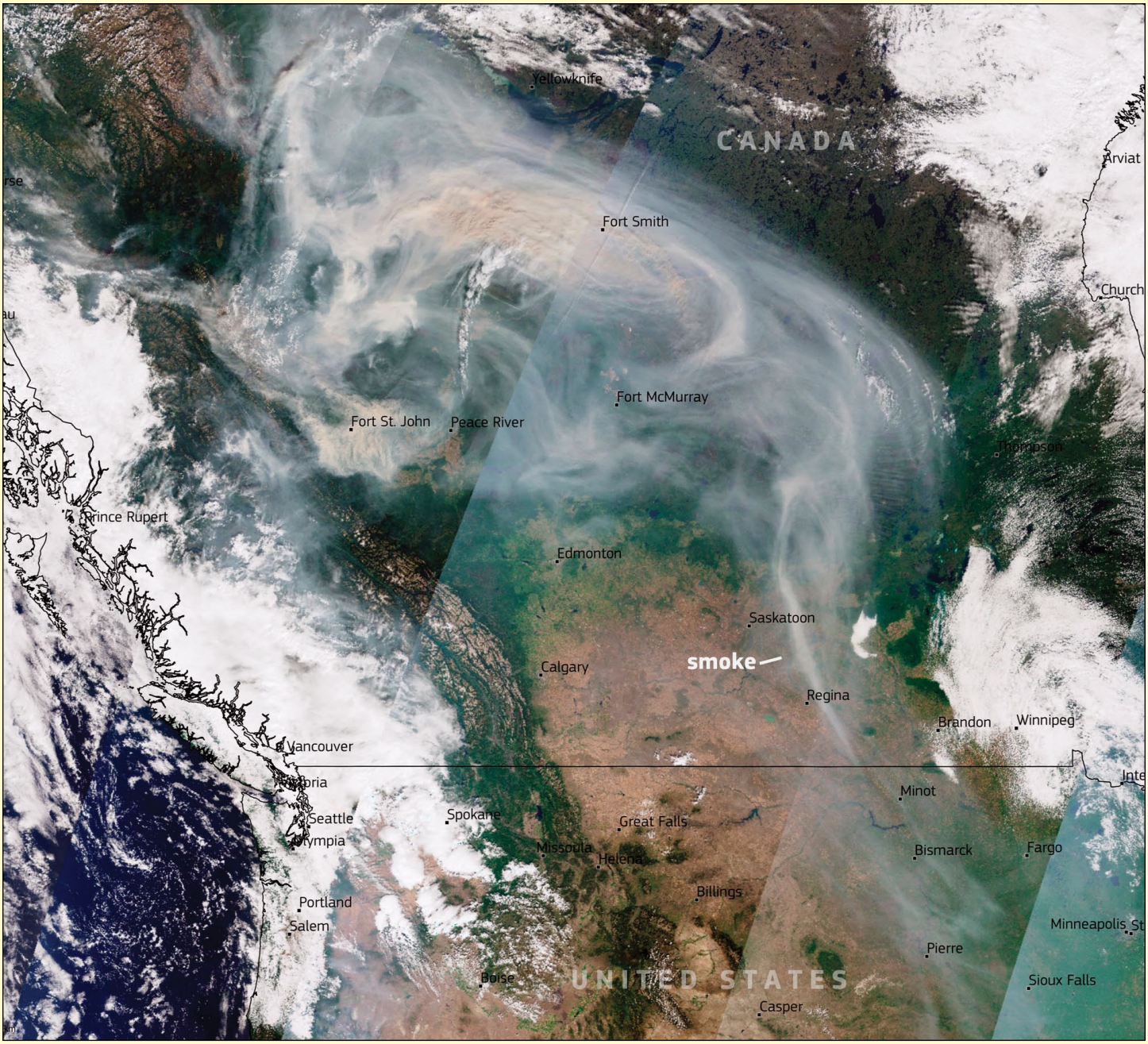

Credit: European Union, Copernicus Sentinel-3 imagery

Wildfires plagued Canada during summer 2023 in the worst wildfire season on record, exacerbating ongoing air quality issues due to dense smoke. The country had been ravaged by fires for three long months, with numerous new blazes rapidly spreading across Alberta, British Columbia, and the Northwest Territories.

The large number of fires generated an immense cloud of smoke that affected air quality in adjacent areas. According to forecasts from the *Copernicus Atmospheric Monitoring Service* (CAMS), the smoke wss travelling long distances, moving from western Canada into the North Atlantic, and by late August had already reached parts of Europe.

This mosaic of images, produced using data from Copernicus Sentinel-3 satellites that were captured on August 29, shows the distribution of smoke, primarily in the areas of British Columbia, Northwest Territories and Alberta, where the fires were then concentrated.

CAMS provides accurate and timely forecasts of air quality on a global scale, assisting in decision-making on health issues arising from large-scale environmental crises such as wildfires.

Atmospheric Rivers Swamp Central Chile

NASA Earth Observatory

Story by Adam Voiland

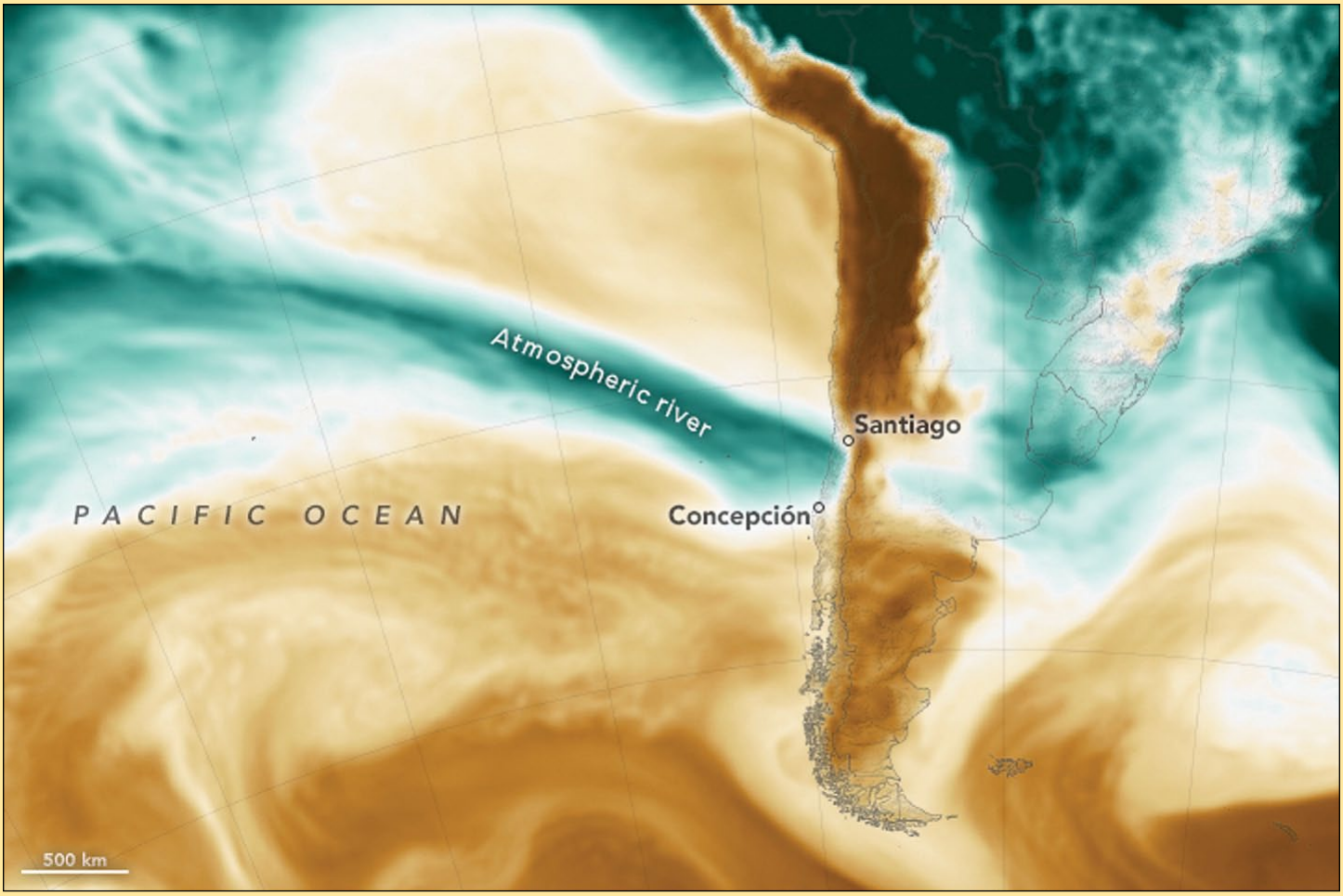

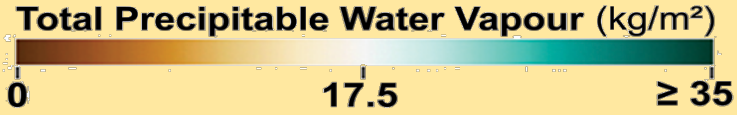

For more than a decade, drought has plagued central Chile. The prolonged dry period—a megadrought—has fuelled wildfires, strained water supplies, and parched crops.

In winter 2023, the region got some relief in the form of two atmospheric rivers that brought hundreds of millimetres of rain and snow to the region. However, too much rain fell too quickly in some areas, prompting floods and mudslides that damaged roads and bridges, destroyed thousands of homes, and displaced tens of thousands of people.

The map above shows the total precipitable water vapour in the atmosphere on August 21, 2023. Precipitable water vapour is the amount of water in a column of the atmosphere if all of the water vapour were condensed into liquid. The image was derived from the *Goddard Earth Observing System* (GEOS), which uses satellite data and models of physical processes to calculate what is happening in Earth's atmosphere, oceans, and land surfaces.

The narrow band of moisture (green) stretching from the central Pacific Ocean to Chile is a signature of an atmospheric river—a long, narrow region that transports vast amounts of water vapour from the tropics poleward. In subtropical Chile, atmospheric rivers contribute 45% to 60% of the annual precipitation, most of it during the winter rainy season (June to September).

El Paico in the Santiago metropolitan region saw nearly 80 millimetres of rain fall between August 19-21, while areas farther inland in the foothills of the Andes saw as much as 370 millimetres of rain, according to *Floodlist*. Meanwhile, some news outlets reported that 2 or more meters (up to 8 feet) of snow fell in high mountain areas.

Some of the worst flooding occurred in the Maule, Ñuble, and Biobío regions of Chile. '*There was a strong orographic effect*,' said atmospheric scientist René Garreaud of Universidad de Chile. '*We saw five to ten times more rain in the Andean foothills compared to Chile's Central Valley.*'

Higher elevation areas saw boosted rainfall totals because the Andes forced the incoming river of moisture upward, where lower air pressure and cooler temperatures cause water vapour to more easily condense into rain droplets on the windward side of mountains. This same effect produces rain shadows on the lee side of mountains.

Several days after the surge of rain, rivers were still swollen and discoloured. Floodwaters can pick up material, such as sediment from riverbanks, that becomes suspended in the water and makes it appear brown. The Moderate Resolution Imaging Spectroradiometer (MODIS) on NASA's Aqua satellite captured an image (below) showing rivers carrying plumes of suspended sediment into the Pacific Ocean on August 26, 2023.

The atmospheric river in August followed a similar event in June. According to Garreaud, the June event delivered more than 500 millimetres of rain over a two-day period to the Maule foothills, roughly double what normally falls in Santiago in a year.

The El Niño developing in the Pacific may be affecting how these events play out. 'We are seeing extra moisture in the central Pacific, but the coupling with the atmosphere is still relatively weak,' stated Garreuad. 'The Pacific anticyclone remains strong, and we haven't yet seen a blocking high to the south of the continent—the typical signature of winter storms that are strongly influenced by El Niño.'

The concept of atmospheric rivers first emerged in the 1990s and has become a topic of growing interest to researchers in recent years. Some research suggests that climate change may be causing atmospheric rivers to produce more rain and shift poleward. One analysis of model projections conducted by a team of scientists at NASA's Jet Propulsion Laboratory found that atmospheric rivers may decrease in frequency but grow longer and wider under a scenario in which future greenhouse gas emissions remain high.

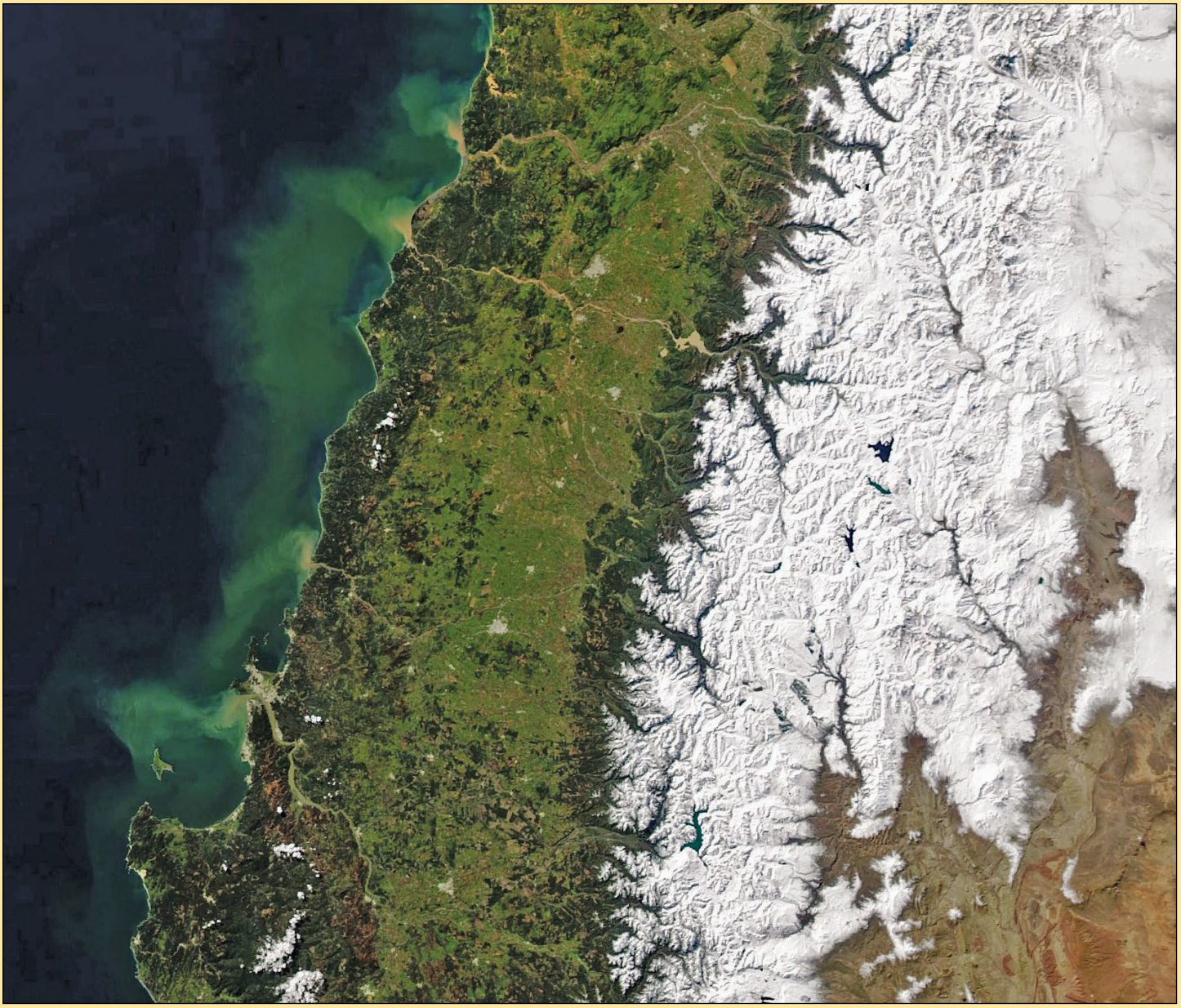

Rivers are seen to be carrying plumes of suspended sediment into the Pacific Ocean on August 26, 2023.

NASA Earth Observatory images by Lauren Dauphin and Wanmei Liang, using GEOS-FP data from the Global Modelling and Assimilation Office at NASA GSFC and MODIS data from NASA EOSDIS LANCE and GIBS/Worldview.

Amur Darya River in Uzbekistan and Turkmenistan

MODIS Web Image of the Day

On September 4, 2023, the Moderate Resolution Imaging Spectroradiometer (MODIS) on NASA's Aqua satellite acquired a true-colour image of a swath of green surrounding the Amu Darya River in Uzbekistan and Turkmenistan.

The Amu Darya River flows from the high Pamir Mountains in central Asia across searing desert and eventually into the Aral Sea. As one of the major rivers in the region it is literally a lifeline—turning deserts green and allowing people, plants, and animals to flourish. In the 1960s, water started to be diverted from the river to expand agriculture and for other uses. While water diversion has successfully expanded agriculture along a wider swath, it has had devastating effects in the 'downstream' section of the river. Both Uzbekistan and Turkmenistan are considered 'downstream'.

A white salt pan can be seen at the upper left (northwest) in this image. To its east is an area of cracked soil, bits of green, and pools of water. This wasted soil marks the southern boundary of the once-thriving Aral Sea. Once an expansive and robust inland sea, the Aral Sea began to die as the water in the rivers that fed it (the Amu Darya and the Syr Darya) began to be diverted, and water flow dwindled. Today, most of the Aral Sea has dried up, leaving nothing behind but parched, hypersaline soils that easily become airborne dust.

Water diversion and cropland expansion also threatens a unique and ecologically vital forest ecosystem. Called 'tugai' or the *Central Asian Riparian Woodlands Ecoregion*, it exists only along large rivers in Central Asian Deserts. The primary locations are along the Tarim River, the Syr Darya, and the Amu Darya. Tugai forest is rich in the Euphrates poplar tree, several species of shrub, along with some grasses. It provides critical habitat for a wide variety of species, especially migratory birds. The hardy and drought-and-heat tolerant vegetation is critical to prevent desertification, provide protection from sandstorms, and protect biodiversity. The green along the Amur Darya still holds a substantial remnant of tugai forest: however, agricultural fields—especially cotton—continue to replace the forest at an expanding rate.

Image Credit: MODIS Land Rapid Response Team, NASA GSFC

Lake Urmia Shrivels Again

NASA Earth Observatroy

Story by Lindsey Doermann

NASA Earth Observatory images by Lauren Dauphin, using Landsat data from the U.S. Geological Survey.

After rapidly growing in volume just a few years earlier, northwest Iran's Lake Urmia dried out almost completely in autumn 2023. The largest lake in the Middle East, and one of the largest hypersaline lakes on Earth at its greatest extent, Lake Urmia has for the most part transformed into a vast, dry salt flat.

On September 7, 2023, the OLI-2 (Operational Land Imager-2) on Landsat 9 captured the left-hand image showing the desiccated lakebed. This stands in contrast to the image from three years earlier (right), acquired by the OLI on Landsat 8 on September 8, 2020, when water filled most of the basin and salt deposits were only visible around the lake's perimeter. That replenishment followed a period of above-average precipitation that sent a surge of freshwater into the basin, expanding its watery footprint. Drier conditions have since brought levels back down.

The longer-term trend for Urmia has been one toward drying. In 1995, Lake Urmia reached a high-water mark: then, in the ensuing two decades, the lake level dropped more than seven metres and fell some 90% in area. Consecutive droughts, agricultural water use and dam construction on rivers feeding the lake have contributed to the decline.

A shrinking Lake Urmia has implications for ecological and human health. The lake, its islands, and surrounding wetlands comprise valuable habitat and are recognised as a UNESCO Biosphere Reserve, Ramsar site, and national park. The area provides breeding grounds for waterbirds such as flamingos, white pelicans, and white-headed ducks, as well as a stopover for migratory species. However, with low lake levels, what water remains becomes more saline and taxes the populations of brine shrimp and other food sources for larger animals.

A shrinking lake also increases the likelihood of dust from the exposed lakebed becoming swept up by winds and degrading air quality. Recent studies have linked the low water levels in Lake Urmia with respiratory health impacts among the local population.

The relative effects of climate, water usage, and dams on Lake Urmia's water level is a topic of debate. The lake did see some recovery during a 10-year restoration program beginning in 2013. However, the efficacy of that effort has been difficult to assess since strong rains also fell during that period. Some research has concluded that climatic factors were primarily responsible for the recovery.

Experiments with IASI Data

Richard Osborne

Background

In previous issues of this newsletter, I have described various methods of visualising derived products that are available over *EUMETCast*. By derived products, I am referring to those which are not direct optical representations of the view from a satellite in the visible and near infrared regions of the spectrum but represent properties such as surface temperature, precipitation levels, atmospheric composition and wind properties.

In this article I am describing my experiments in visualising products derived from the *Infrared Atmospheric Sounding Interferometer* (IASI) which is described as the most advanced instrument present on the Metop series of satellites. It can determine trace atmospheric gases, land/sea surface temperatures, cloud properties and can also provide temperature, humidity and trace gas profiles from the surface into the stratosphere with a vertical resolution of one kilometre. However, this article is concentrating on methods to visualise the data rather than an examination of the technical capabilities of the instrument which can be found elsewhere. I also cover a discovery that I made about the inner workings of one of the most popular visualisation applications.

Data Sources

The IASI data is available via *EUMETCast* over two different channels. One channel is dedicated to the transmission of global IASI data using the BUFR file format. A series of files for a single granule is provided where, for example, each trace gas and the temperature/humidity products are provided as separate files. The other channel is the *Regional Data Service/EARS,* which is used to provide near real time data via a series of ground stations with minimum latency. For some reason, the latter channel uses the HDF file format and only one file is provided for a single granule with a subset of the data products available on the global channel. One curious difference between the channels relates to the number of samples in the vertical profiles. The BUFR files represent 101 vertical atmospheric profiles whereas the HDF files have 138.

Because of the addition of a height element in these profiles, the relevant data is packaged in three dimensional (3D) data arrays which adds an extra dimension (literally) to the normal practice of visualising 2D arrays with simple latitude and longitude coordinates. One way of thinking about the temperature and humidity profiles is as a series of horizontal 2D arrays that are stacked one on top of another.

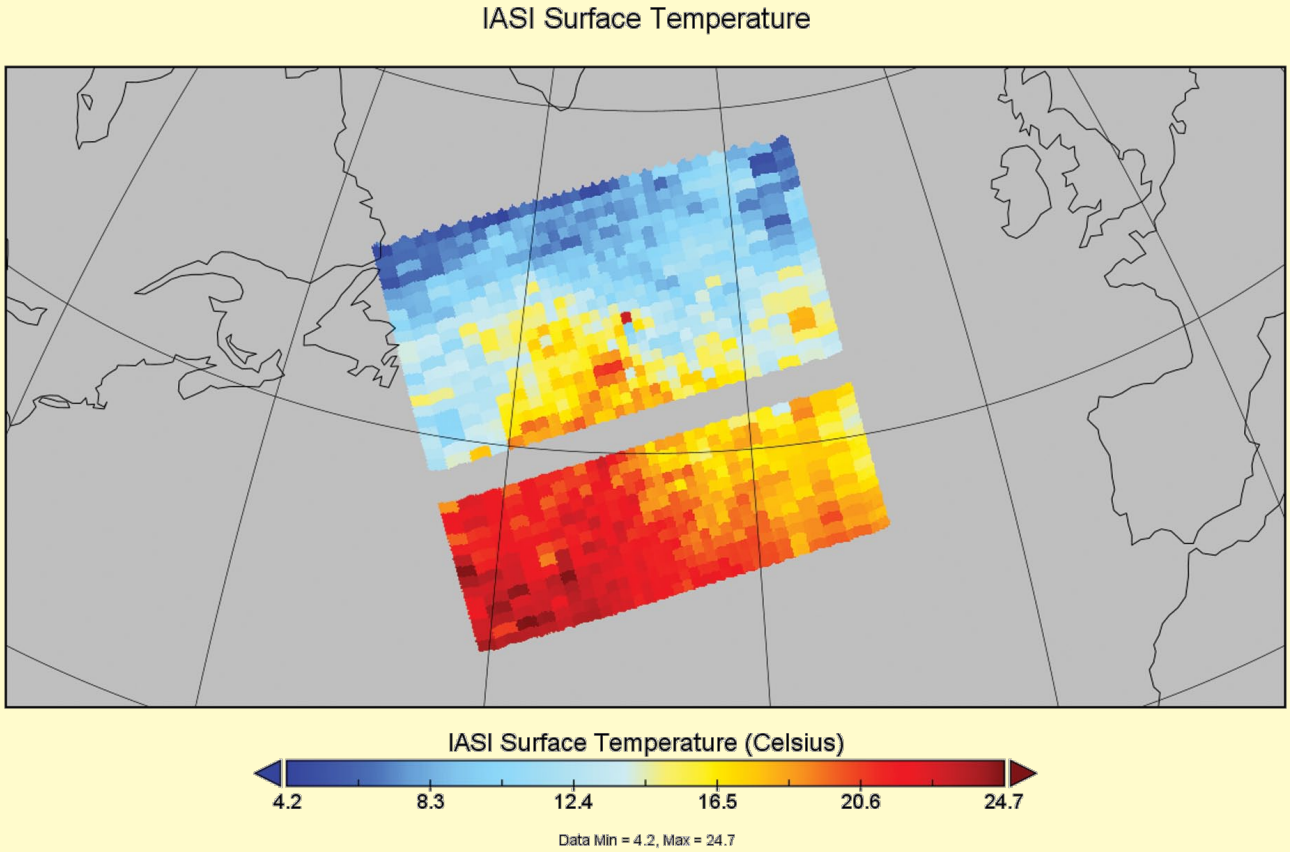

Figure 1 - IASI Surface Temperature Plot using Panoply from HDF file. The gap is caused by missing scan lines in the dataset

From a visualisation point of view, I was looking for an easy way to select and display a given 2D array within the stack and also to plot a profile in the vertical direction showing how temperature varies with height.

Viewing IASI HDF Files

Because a number of generic viewers already exist that can handle HDF files (GEO Newsletter No 72, page 38), I decided to check these first to see if they could handle the 3D nature of the dataset, thereby avoiding the need for additional coding. Of all the ones that I tried, only *Panoply* was able to handle the 3D nature of the dataset natively and allow selection of a specific layer in the temperature and humidity profiles. Also, *Panoply* could generate a 2D colour contour map from any two of the three axes in a 3D dataset which provided a means to plot a profile in a vertical direction. Figure 1 shows a *Panoply* plot of IASI surface temperature which is a standard 2D dataset. Figure 2 shows the along-track vertical temperature profile related to the horizontal plot in Figure 1. The axis units correspond to the co-ordinates of the underlying dataset and do not represent physical values such as height or distance, the determination of which is beyond the scope of this article.

Merging IASI HDF Files

As mentioned previously, the *Regional Data Service/ EARS* uses multiple ground stations in succession to receive data from the satellite as it goes past each one. For each station, the full dataset derived from a satellite pass is then transmitted over *EUMETCast* as a single file.

As *Panoply* can only display the data from two files at any given time, my goal was to merge these individual datasets into one file so that *Panoply* could display a composite image derived from all applicable stations.

To merge the files, I concluded that the simplest method, which also provided the greatest control, was to use *Python* and the *Numpy* library in particular. (The *Numpy* library allows the creation and manipulation of multi-dimensional data arrays). I converted the datasets from the individual received files into *Numpy* arrays, combined them and saved the result as a single HDF file which could be ingested and displayed by *Panoply*. Unfortunately, the result was not satisfactory as the resultant image contained jagged geometrical artefacts which were clearly not relevant. After some research, I think that I have identified the reason.

Figure 3 shows a *VISAN* plot of the IASI surface temperature using exactly the same dataset as Figure 1. However, *VISAN* uses a scatter plot technique where every data point is represented by a dot and located exactly at the associated latitude and longitude co-ordinates. Each data point is plotted in isolation and is not affected by the presence of any other data point. The pattern of dots in the plot is a feature of the IASI instrument.

Panoply, on the other hand, attempts to infill the space between data points which are adjacent in the underlying data array with solid colour at all levels of zoom, giving a pleasing visual effect. Close examination of Figure 1 will reveal the infill when compared with Figure 3.

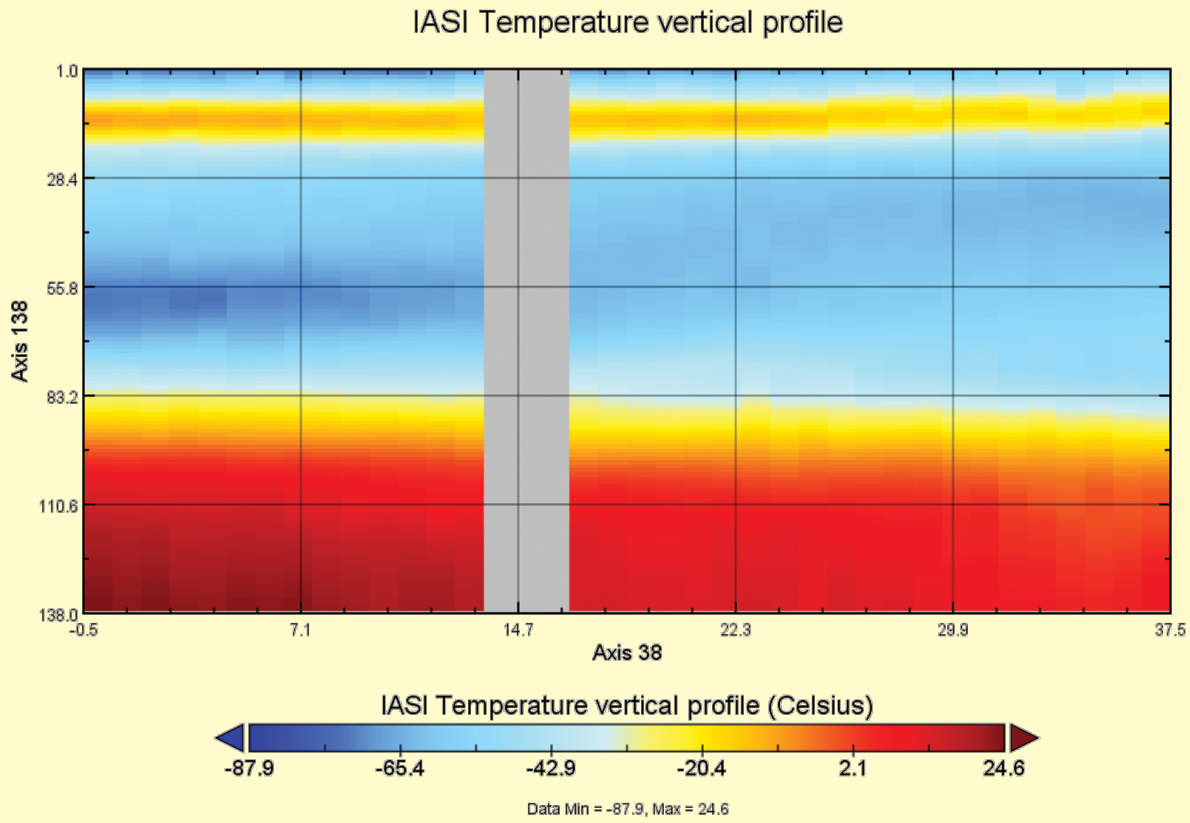

Figure 2 – IASI Vertical Temperature Profile showing temperature variation from surface to upper atmosphere going from North to South

However, if there is a jump in latitude and/or longitude co-ordinates between adjacent data points, it seems that *Panoply* gets confused and infills with solid colour between data points, even if they have a significant geographical separation. Normally, an unmodified dataset would not have these jumps so the problem does not appear. However, I had combined two or more datasets with overlapping geographical areas of coverage so there was a jump at the boundary between them.

The obvious answer was to eliminate the overlaps by detecting and removing duplicated information so that there was a smooth geographical co-ordinate transition from one dataset to another. However, this proved not to be simple as there was a very small numerical difference between the dataset provided by one station when compared to another, even though they were receiving data at the same time from the same satellite. This meant that identifying duplicate data was not a trivial task. I decided to try and bypass this obstacle by deriving a timestamp for each scan line and checking for duplicates before removing the duplications. This appeared to work at first but ultimately proved doomed to failure as one station randomly dropped scan lines from their dataset. At this point I gave up.

Viewing IASI BUFR Files

The global IASI coverage datasets are transmitted as BUFR files with nine separate files for each granule which represents a defined area of geographical coverage. These include cloud parameters, trace gases and temperature/ pressure profiles.

My first attempt to display the IASI BUFR files used BUFRdisplay as described in my BUFR article featured in GEO Newsletter No 79. Unfortunately, *BUFRdisplay* failed with an error on two of the BUFR file types. I eventually traced the problem to an obscure BUFR descriptor called 'add associated field' which *BUFRdisplay* could not process properly in this context (BUFR can be a fiendishly complicated protocol at times). To handle these two file types, I required a different approach.

I have previously described how I used *Python* to extract variables from a BUFR file in the form of *Python Numpy* arrays. Having already demonstrated that *Panoply* can display IASI data in the form of an HDF file, the obvious process was to convert the wanted data from the BUFR file into an HDF5 file via *Python Numpy* arrays which proved to be a fairly simple affair.

There are other potential methods of visualising the data such as the *VISAN* application or the *matplotlib Python library* but I have not pursued this route. Incidentally, *SatPy* has a limited number of experimental readers for derived products including the IASI HDF5 format and IASI SO2 data in BUFR format.

I have also merged the datasets from multiple BUFR files using the process described in the previous section to display multiple granules at the same time. Fortunately, individual BUFR file sets abut in their geographical coverage so I had no problem with spacial overlapping.

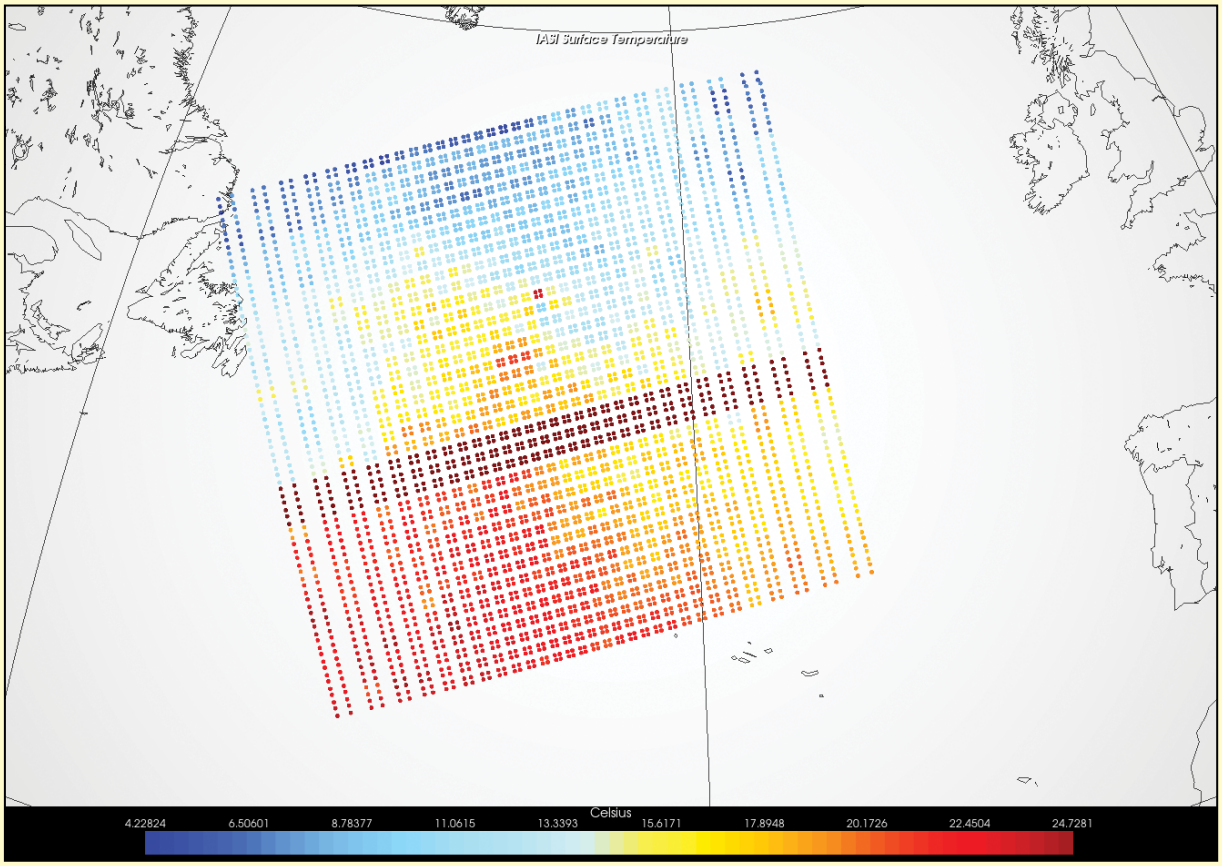

Figure 3 - IASI Surface Temperature Plot using VISAN from HDF file. Input data is identical to that used in Figure 1.

Darkened by the Moon's Shadow

NASA Earth Observatory

Story by Emily Cassidy

The DISCOVR image showing the darkening over the USA caused by the annular eclipse

NASA image courtesy of the DSCOVR EPIC team. NASA Scientific Visualization Studio map by Michala Garrison

On October 14, 2023, the Moon aligned with the Sun and Earth to produce an **annular solar eclipse**. The spectacle bathed millions of Americans in a lunar shadow as the Moon blocked the Sun's rays.

An annular eclipse occurs when the Moon passes in front of the Sun but is too distant from Earth to completely obscure it. The Moon is at or near its farthest distance from Earth—known as its apogee—during an annular eclipse, making it look smaller in the sky. This leaves the Sun's edges exposed in a red-orange ring, dubbed the 'ring of fire'. A satellite caught this earthly view of the event, as the Moon's shadow crossed North America.

The above image was acquired during the eclipse by NASA's EPIC (Earth Polychromatic Imaging Camera) imager aboard DSCVR (Deep Space Climate Observatory), a joint NASA, NOAA, and U.S. Air Force satellite. The sensor provides frequent global views of Earth from its position at Lagrange Point No 1, the gravitationally stable point between the Sun and Earth, about 1.5 million kilometres from Earth. In this view, acquired at 16:58 UT, the shadow, or umbra, from the Moon can be seen falling across the southeastern coast of Texas, near Corpus Christi.

While the annular eclipse was partially visible across the entire United States, Mexico, and countries in Central and South America, the path of annularity—where the largest area of the Sun was covered by the Moon from the observers' point of view—was the best place to view it.

The path of annularity across the United States on October 14

The map above, developed by NASA's Scientific Visualization Studio, shows the dark path of the annularity stretching across the lower 48 states from Oregon to Texas. The map uses data sets from several NASA missions. Imagery from MODIS (Moderate Resolution Imaging Spectroradiometer) instruments on the Terra and Aqua satellites was the source of the Blue Marble Next Generation composite used to depict the terrain.

The path of annularity started in Oregon around 9:13 a.m. Pacific Daylight Time, though cloudy skies blocked the view for some sky watchers. The shadow then moved southeast across Nevada, Utah, Arizona, Colorado, and New Mexico, before passing over Texas and the Gulf of Mexico.

Also visible on the map within the path are duration contours. These delineate the length of time annularity lasted. The closer to the centre of the solar eclipse path, the longer it lasted. For the annular path, times range from a few seconds on the outer edge to a maximum of around 4.5 minutes in the centre.

Ring of Fire

The official NASA broadcast of this annular eclipse, which followed the event throughout its entire hour and three quarters duration, can be viewed at the following URL:

https://www.youtube.com/watch?v=oUg22TRWGdI

The next annular solar eclipse visible from the United States will not occur until June 21, 2039. But a total solar eclipse will darken skies from Texas to Maine on Monday, April 8, 2024.

Record-setting Snow in Alaska

MODIS Web Image of the Day

A thick layer of newly-fallen snow shone brightly across south-central Alaska on November 14, 2023, when the Moderate Resolution Imaging Spectroradiometer (MODIS) on NASA's Aqua satellite acquired this true-colour image. Sunlight reflecting off the snow appears intensely white—much whiter than the clouds crossing the scene. Mountainous terrain creates blue-tinted shadows on the brilliant white snow. Cloud hangs over the Cook Inlet as well at the city of Anchorage, which is located at the head of Cook Inlet.

By Mid month, Anchorage had received a total of 96.3 cm of snow, close to the city's all-time record November snowfall of 98.6 cm. One snowstorm alone delivered a whopping 46 cm to the city between November 8-9.

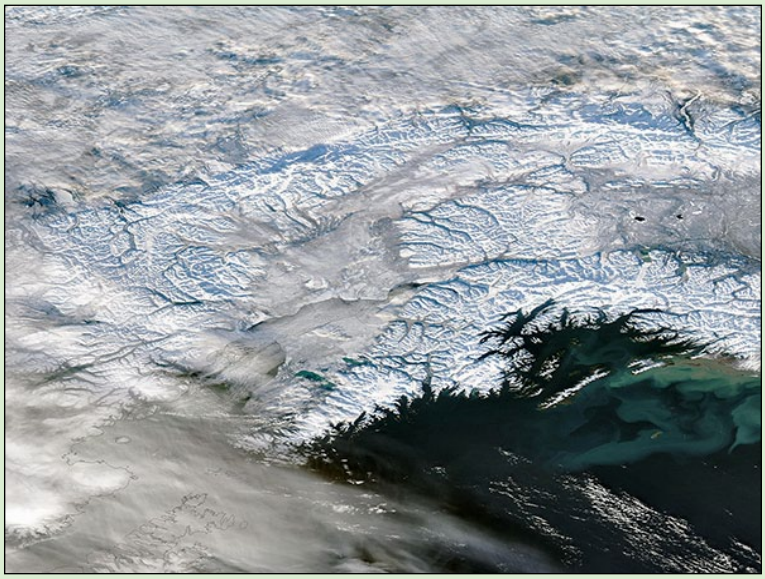

Credit: MODIS Land Rapid Response Team, NASA GSFC

Getting the best from Meteor M 2-3 GIS Infrared Images

Les Hamilton

By the time you read this, Northern Hemisphere daylight will be very much reduced. Consequently, colour composite Meteor M 2-3 images produced by the *MeteorGIS* software using the two visible light channels will be under-illuminated and disappointingly dark. Now is the time to make the most of the satellite's infrared transmissions which are generally at their incisive best during the cold of months of December and January.

Previous satellites in the Meteor 2M series all transmitted infrared LRPT imagery during the winter months via the 10.5 - 11.5 μm *Thermal-infrared band* transmitted on channel 5. But Meteor M 2-3—currently at least—is instead transmitting its infrared data in the 3.5 - 4.1 μm *Mid-infrared band* on channel 4.

This is a problem, because *MeteorGIS* has been hard coded to process infrared imagery received on channel 5 only. Hopefully there may eventually be an update to cater for channel 4. But currently, *MeteorGIS* simply just does not 'know' how to process this channel 4 data, and its attempts are disappointing to say the least.

Figure 1, centred over the British Isles, was received from an ascending Meteor M 2-3 pass on the evening of November 24, 2023, when much of England experienced sub zero temperatures.

The image is very dark and its histogram displays only an extremely narrow range of tones concentrated in the 'dark' end of the spectrum, illustrated in figure 2. This image can, of course, be stretched across the entire range by means of external software such as *Photoshop* or *GIMP*, and figure 3 shows the result. This reveals yet another problem: the image has been rendered in negative.

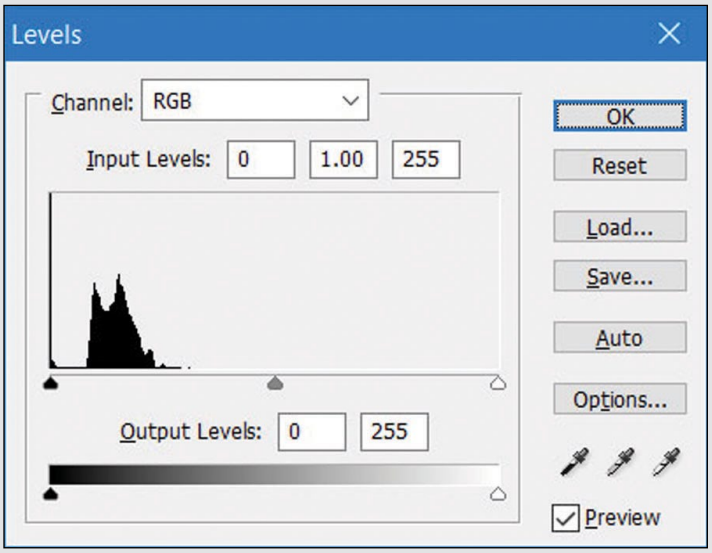

Figure 2
The limited range of greyscale levels present in Figure 1

Figure 1
This is how MeteorGIS processed the Channel 4 data stream during an overnight pass of Meteor M 2-3 at 20:38 UT on November 24, 2023

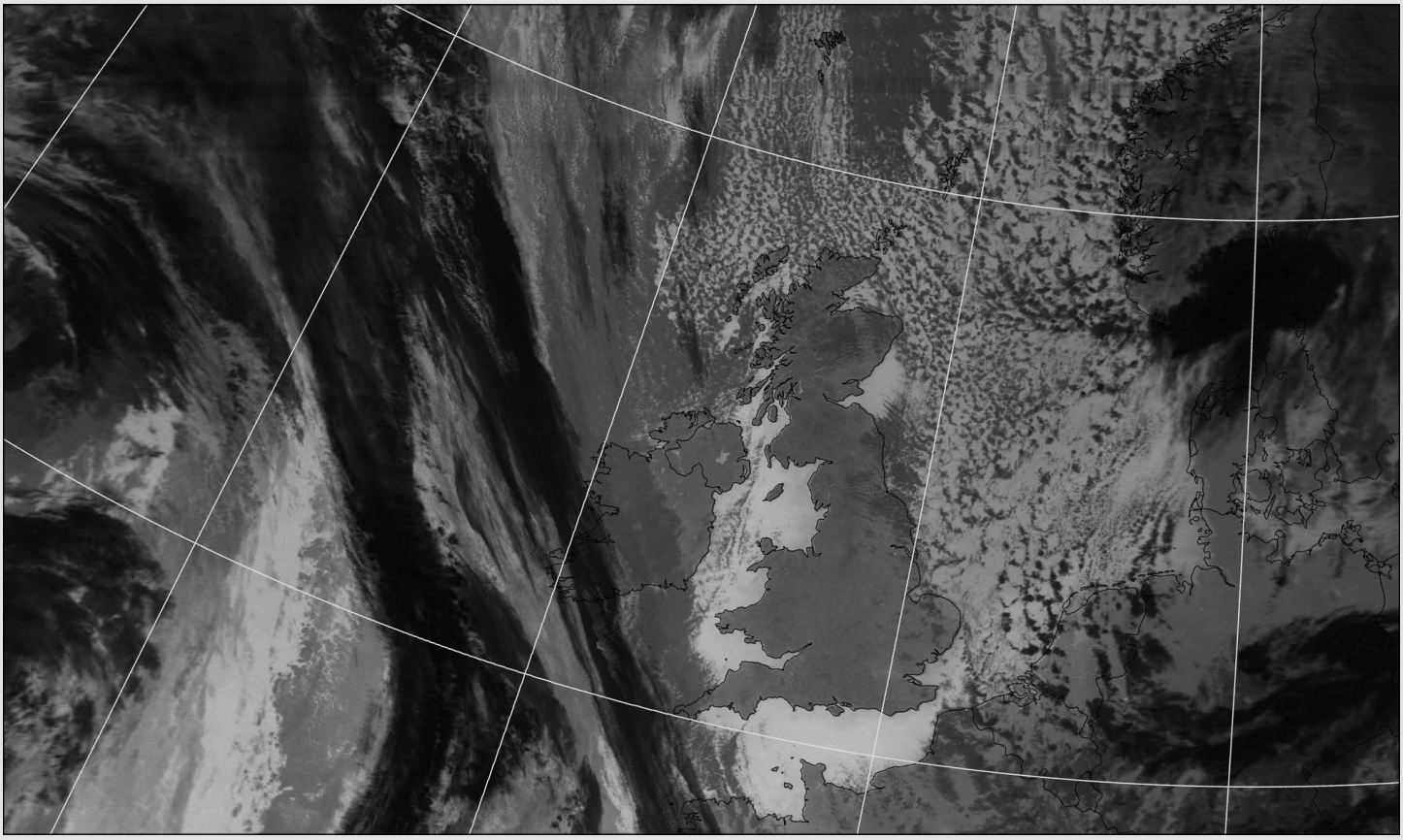

Figure 3 - The Channel 4 image after stretching the greyscale

The cold cloud tops are displayed in shades of black through dark grey (denoting warmth) while the warmer seas and land areas are rendered in lighter shades of white through grey (cold). You might argue that all that is now necessary is to invert the greyscale, but the outcome is still disappointing: the image just does not contain sufficient grey levels to do the scene justice.

The Solution

Meteor M 2-3 has the ability to transmit any three from its six LRPT channels simultaneously: channels 1-3 carry visible light data while channels 4-6 carry infrared data. The image datafiles saved in the *Images_M2* folder after acquiring this transmission from the satellite are shown in figure 4. The final number of each designator string is a code denoting from which channel it originated: channels 1 to 6 are denoted by the numbers 64 through 69. The channel 4 image therefore ends in '67', illustrated in red opposite.

It is clear that channels 1, 2 and 4 were being transmitted, although, as an overnight transmission, channels 1 and 2 did not, of course, contain image data in this example.

Creating a Pseudo Channel 5 Image

Although channel 5 data from Meteor M 2-3 were completely lacking in this transmission, it is possible to 'deceive' *MeteorGIS* into processing the image data as though it were from channel 5.

The secret is simple: just edit the filenames and replace the '**67**' designator by '**68**' (figure 5). To achieve this, right-click on a filename, select 'Rename' from the drop-down menu, make the change, then press 'Return' to confirm.

2023-11-11-20-44-21-384_64.bmp
2023-11-11-20-44-21-384_64.stat
2023-11-11-20-44-21-384_65.bmp
2023-11-11-20-44-21-384_65.stat
2023-11-11-20-44-21-384_67.bmp
2023-11-11-20-44-21-384_67.stat
2023-11-11-20-44-21-384_123.jpg
2023-11-11-20-44-21-384_123.jpg.gcp
2023-11-11-20-44-21-384_123.jpg.stat

Figure 4
The original image datafiles saved in the Images_M2 folder

2023-11-11-20-44-21-384_64.bmp
2023-11-11-20-44-21-384_64.stat
2023-11-11-20-44-21-384_65.bmp
2023-11-11-20-44-21-384_65.stat
2023-11-11-20-44-21-384_68.bmp
2023-11-11-20-44-21-384_68.stat
2023-11-11-20-44-21-384_123.jpg
2023-11-11-20-44-21-384_123.jpg.gcp
2023-11-11-20-44-21-384_123.jpg.stat

Figure 5
The pseudo channel 5 files in the Images_M2 folder

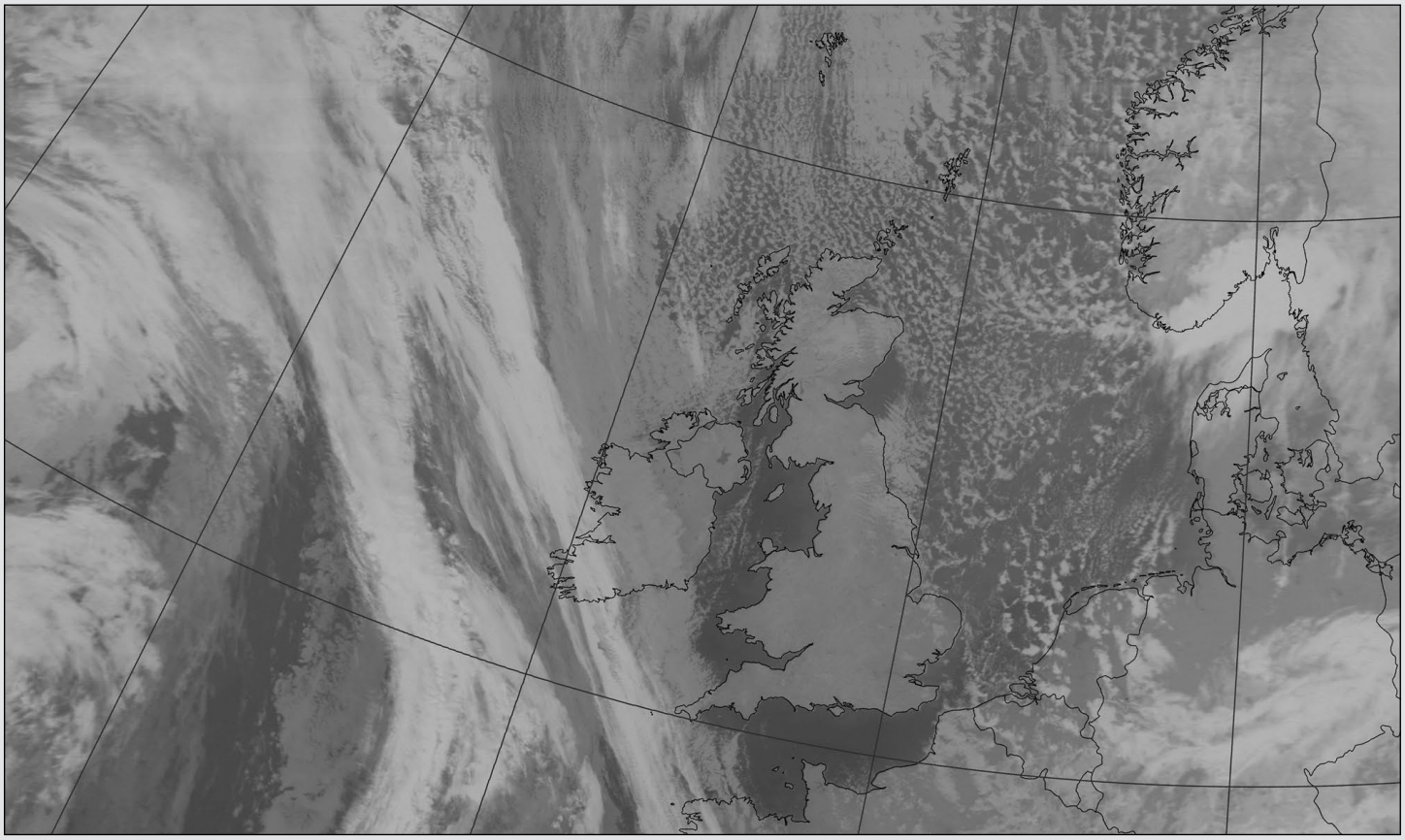

Figure 6 - The Channel 4 image after processing it as a Channel 5 image

Now process these files again as follows

1 Delete any files from the MeteorGIS *FinalImages* folder, as MeteorGIS will not overwrite existing files.

2 Locate the **default.bat** file inside the MeteorGIS/ MeteorGIS **sub** folder and run it by double-clicking it.

3 MeteorGIS will spring into life and the infrared file will now be processed as if it were from channel 5.

4 Once processing is complete, the infrared image will be found in the *FinalImages* folder.

The processed file in our example is shown in figure 6.

This image, though somewhat on the light side, is a big improvement. The greyscale has now been applied correctly to render the cold cloud tops in shades of white and light grey, while the exposed sea and land surfaces are displayed in darker shades of grey.

The 'Levels' histogram for this image (figure 7) now shows a much improved range in the greyscale tones, though they by no means cover the entire spectrum. To complete our task, we must stretch these across the complete range as illustrated in figure 8.

For this final step you require a high-end image processor. If you have *Photoshop*, this is ideal. If not, download and use the *GNU Image Manipulation Program* (GIMP) from

https://www.gimp.org/

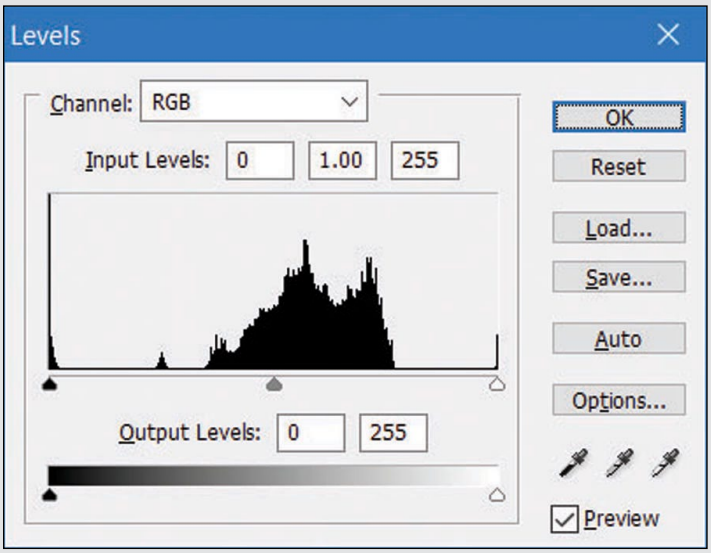

Figure 7 - The greyscale levels present in Figure 6

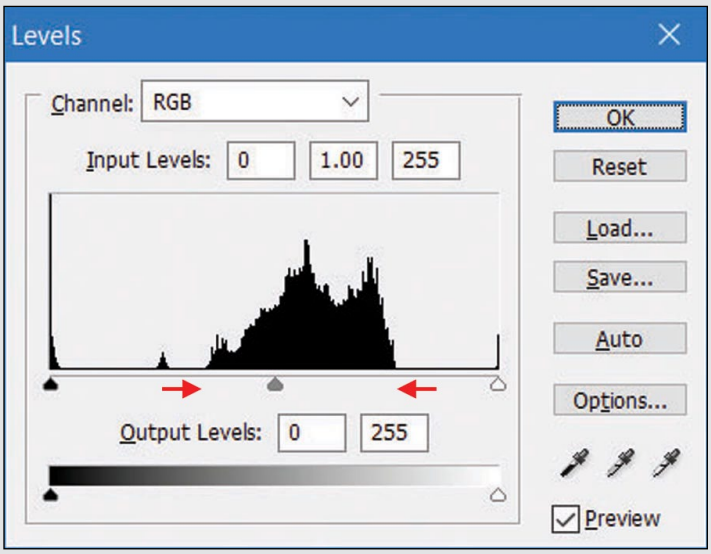

Figure 8 - Stretching the greyscale

Histogram Stretching with Photoshop

- Load the infrared image (figure 6)
- Select: Image —> Mode —> Greyscale
- Select: Image —> Adjust —> Levels

In the 'Levels' panel that pops up over the image, use the mouse to drag the **black triangular marker** at left and the **white triangular marker** at right towards the edges of the histogram This is illustrated by the red arrows in figure 8.

Press 'OK' to confirm, and re-save the image.

Histogram Stretching with GIMP

- Load the infrared image (figure 6)
- From the menubar select: Colors —> Levels

In the 'Levels' panel that appears (figure 9), adjust the markers below the 'Input Levels' window towards the edges of the histogram, click 'OK' and re-save the image.

The above are by no means exclusive, and there are undoubtedly other software packages that can be used.

The final, stretched image is shown below in figure 10, a vast improvement on the original one that resulted when *MeteorGIS* was left to its own devices in dealing with the channel 4 data.

And don't forget that even daytime infrared images from Meteor M 2-3 during the winter months can often reveal much improved detail about advancing weather systems than the poorly illuminated visible images. Do give it a try: you may be surprised just how good these infrared images can be.

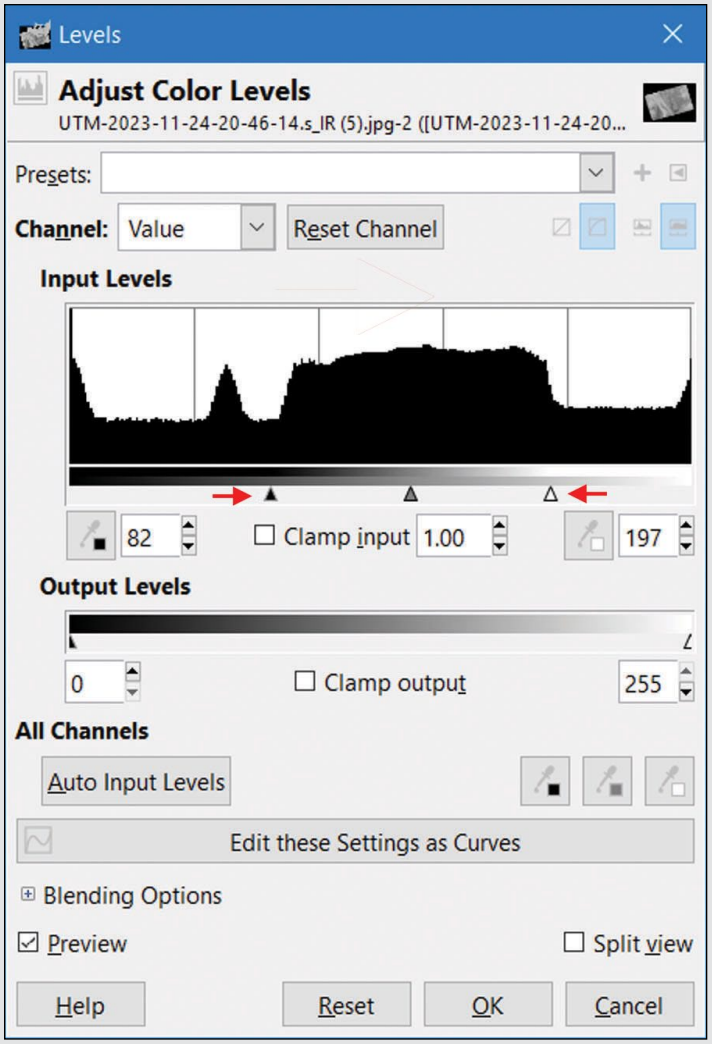

Figure 9 - Stretching the greyscale histogram using GIMP

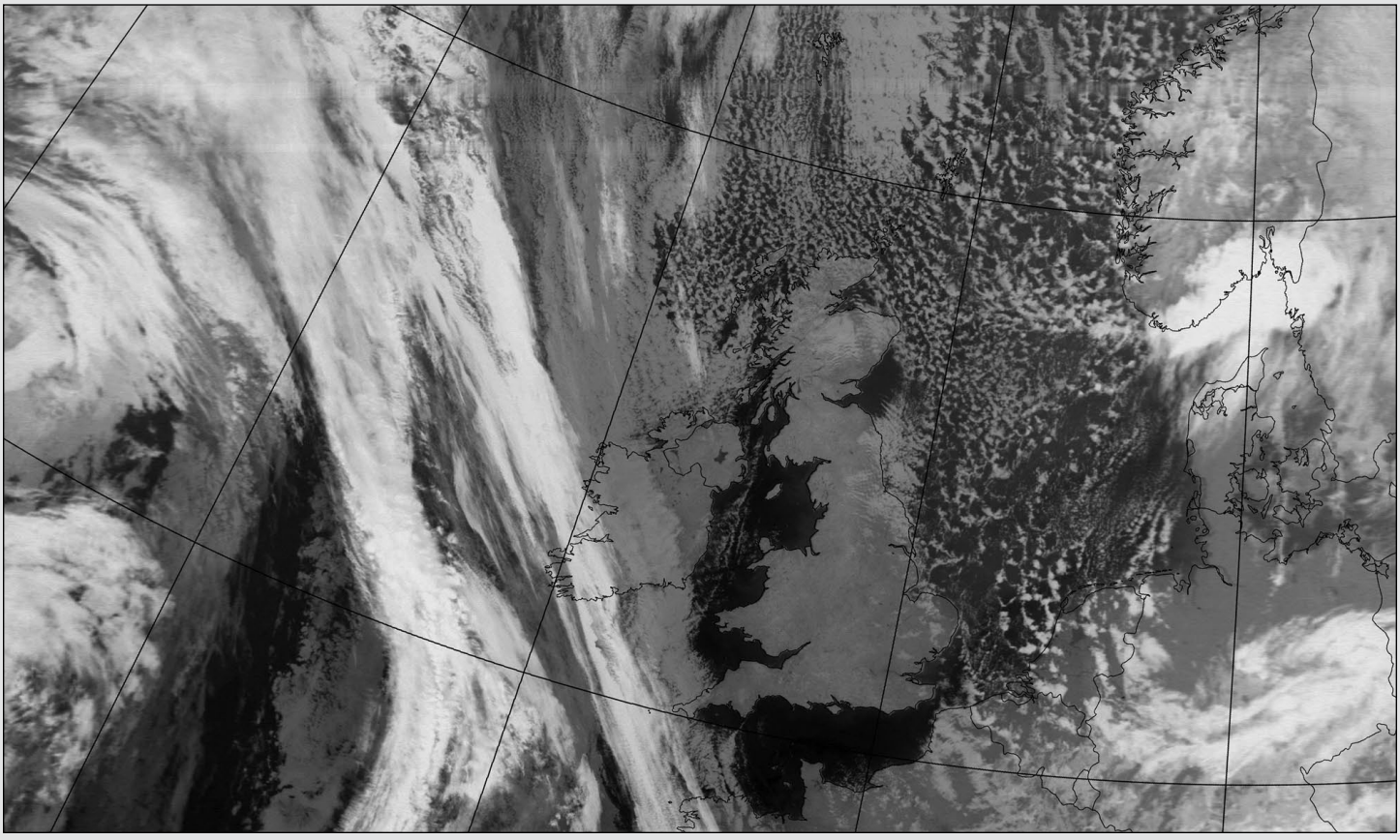

Figure 10

This is the final infrared image, processed as if it were disseminated on channel 5, and stretched.

Restless Kamchatka Volcanoes

NASA Earth Observatory

Story by Lindsey Doermann

NASA Earth Observatory image by Wanmei Liang, using Landsat data from the U.S. Geological Survey

Neighbouring volcanoes on Russia's ever-fiery Kamchatka Peninsula puffed away in mid-October 2023. The OLI (Operational Land Imager) on Landsat 8 captured this image of eruptions in action on October 16. The peaks cast shadows on the snow as the Sun traversed low in the autumn sky.

Visible at the top of the image, the stratovolcano Klyuchevskoy, Eurasia's tallest active volcano, sent a small plume of gas, steam, and possibly some ash wafting to the northeast. The shadow of the mountain's clear conical shape and rising plume offers a sense of three-dimensionality to the view.

In June 2023, the *Kamchatka Volcanic Eruption Response Team* (KVERT) reported the start of Strombolian eruptions at Klyuchevskoy, and in July, a new lava flow was detected on its southeast flank. Explosive eruptions continued in the ensuing months. Varying amounts of ash were sent aloft with gas and steam, at times causing the aviation colour code to be elevated to orange, the third level on a four-colour scale. Activity ramped up in the days before this image was acquired: increasing amounts of lava flowed down the volcano's flanks, and incandescent materials rocketed up to 300 metres above the crater rim.

Farther south, Bezymianny also spewed a volcanic plume, though it is more difficult to discern because of the cloud bank in this scene. KVERT noted an increase in activity at this volcano on October 16, when debris avalanches rushed down the slopes of the lava dome and ash was blown about 70 kilometres northeast of the volcano.

Located along the Pacific Ring of Fire, the Kamchatka Peninsula is a land of volcanoes, home to more than 300 of them. The frequently active Klyuchevskaya range, part of which is shown in this image, is a common locale for geological drama visible from space.

Bushfires in Queensland

NASA Earth Observatory

Story by Emily Cassidy

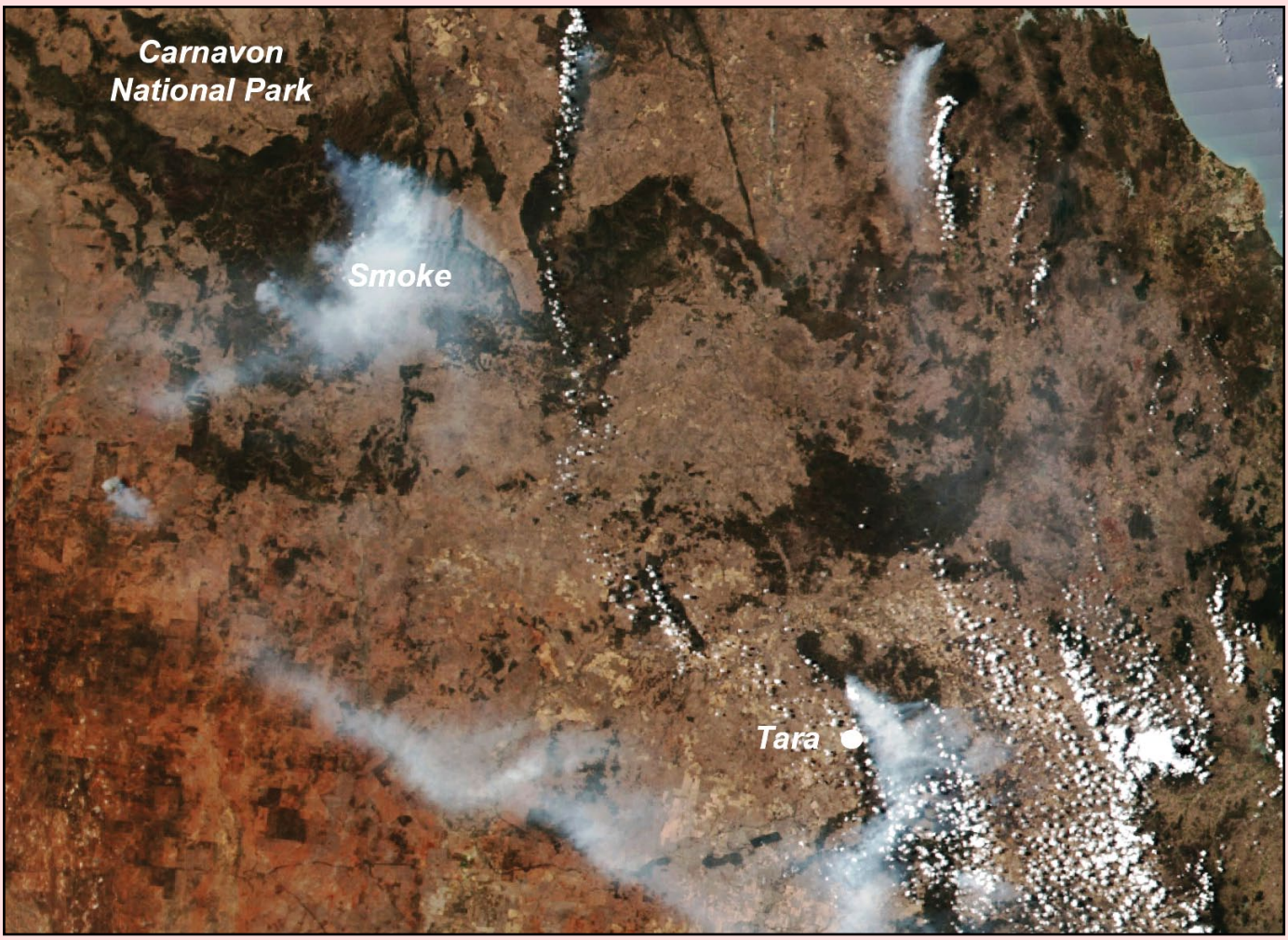

Figure 1 - A Suomi NPP satellite image showing smoke from live bush fires
NASA Earth Observatory image by Wanmei Liang, using VIIRS data from NASA EOSDIS LANCE, GIBS/Worldview, and the Suomi National Polar-orbiting Partnership

Soaring temperatures and dry winds fanned the flames of over 20 bush fires raging in Queensland, Australia in late October 2023. Residents were evacuated from the town of Tara, where homes were destroyed in the blazes.

Figure 1, acquired by the VIIRS (Visible Infrared Imaging Radiometer Suite) sensor on the Suomi NPP satellite, shows smoke from several fires burning in southeastern Queensland on October 24, 2023. On the same day, temperatures reached 40 degrees Celsius, some of the highest on record for the region on that date.

A fire burning in northeast Tara destroyed 16 homes and 11,000 hectares of bushland, according to news reports. Tara has a population of about 2,000 people and is within Western Downs, a fruit-growing region about 250 kilometres west of the state capital Brisbane. Although the emergency evacuation order for the town was lifted on October 26, Queensland Fire and Emergency Services told residents that it was not safe to return to their homes.

Smoke also billowed from the forested Carnarvon Gorge section of the Carnarvon National Park. The fire, active since late September, has been burning on the plateaus above the gorge, which features towering sandstone cliffs, diverse flora and fauna, and Aboriginal rock art.

Figure 2, acquired by the OLI-2 (Operational Land Imager-2) on Landsat 9 on October 21, shows a burn scar from the fire, which has blazed through at least 31,000 hectares of land as of mid-October. According to news reports, protections had been put in place to prevent damage to Indigenous rock art in the park, which was closed until November 13, 2023.

Hot and dry conditions descended on much of Australia during the southern hemisphere's spring, leaving the country at a heightened risk for bush

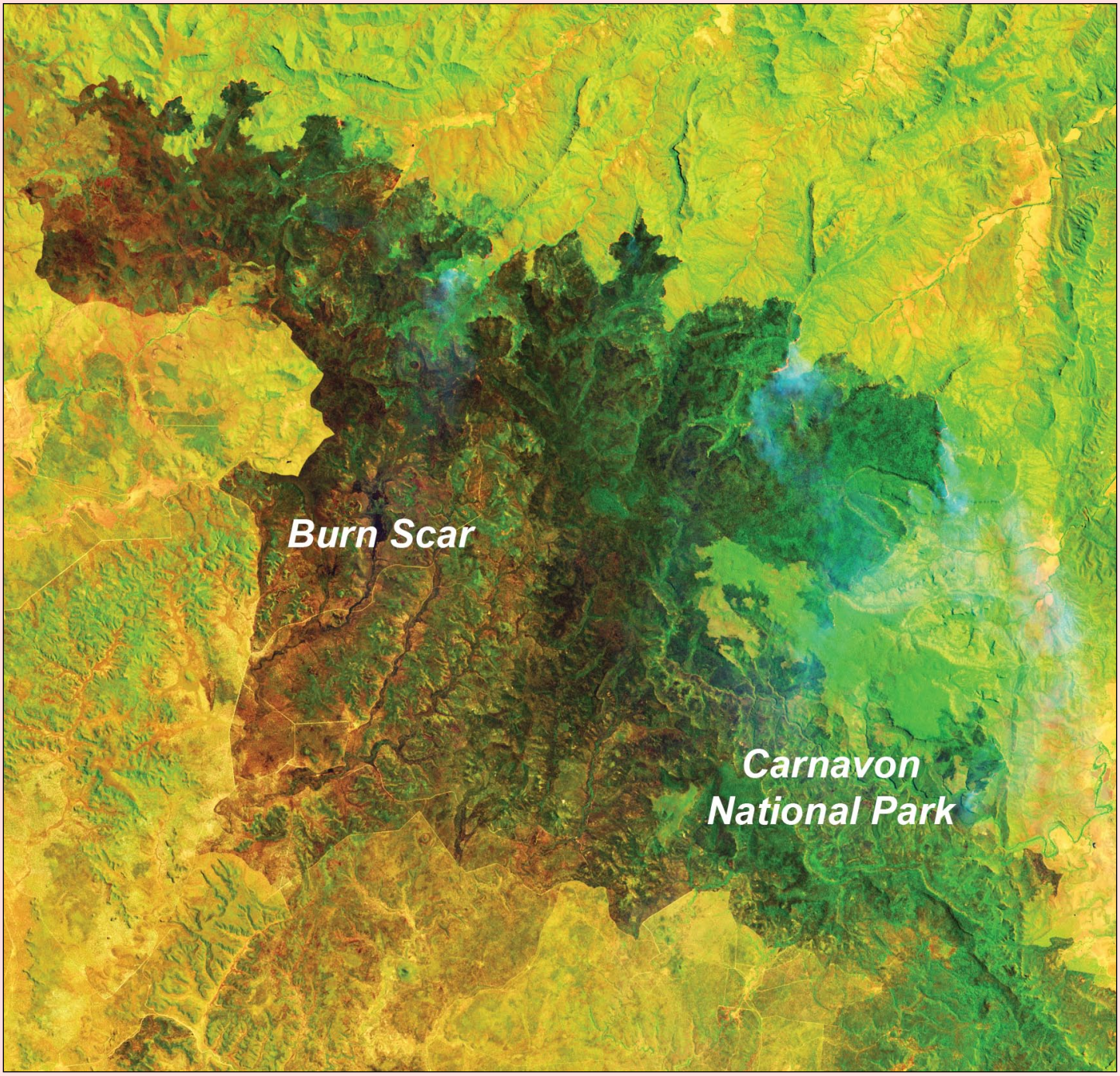

Figure 2 - The Operational Land Imager-2 on Landsat 9 on October 21, imaged a burn scar from the fire
NASA Earth Observatory image by Wanmei Liang, using Landsat data from the U.S. Geological Survey.

fires. Rainfall in September 2023 was 71% below the 1961–1990 average for the country, the driest September on record since 1900. Forecasts by Australia's Bureau of Meteorology expect that November to January rainfall would probably be below average across much of western, southern, and northeastern Australia.

The *Australasian Fire Authorities Council* (the council for fire services in Australia and New Zealand) predicted an increased risk of springtime bush fires, especially in the central and eastern parts of Australia. The council noted that plentiful rainfall from three consecutive La Niña years had built up vegetation in rangelands. Now, the return of El Niño, on top of human-caused warming, is contributing to warm and dry conditions that allow plants to dry out and fuel fires. El Niño typically leads to reduced rainfall in the spring for eastern Australia, and warmer days for the southern two-thirds of the country.

Some of the world's largest and fastest spreading fires burn in the grasslands and shrub lands of Australia, according to a database chronicling the dynamics of 13.3 million fires observed by NASA's MODIS (Moderate Resolution Imaging Spectroradiometer) instruments between 2003 and 2016. The largest fire in the record followed the 2007 La Niña and,w according to the authors of the database, similar large fires in arid regions of South Africa and Australia have typically followed La Niña years.

Remnants of Catastrophic Hurricane Otis

MODIS Web Image of the Day

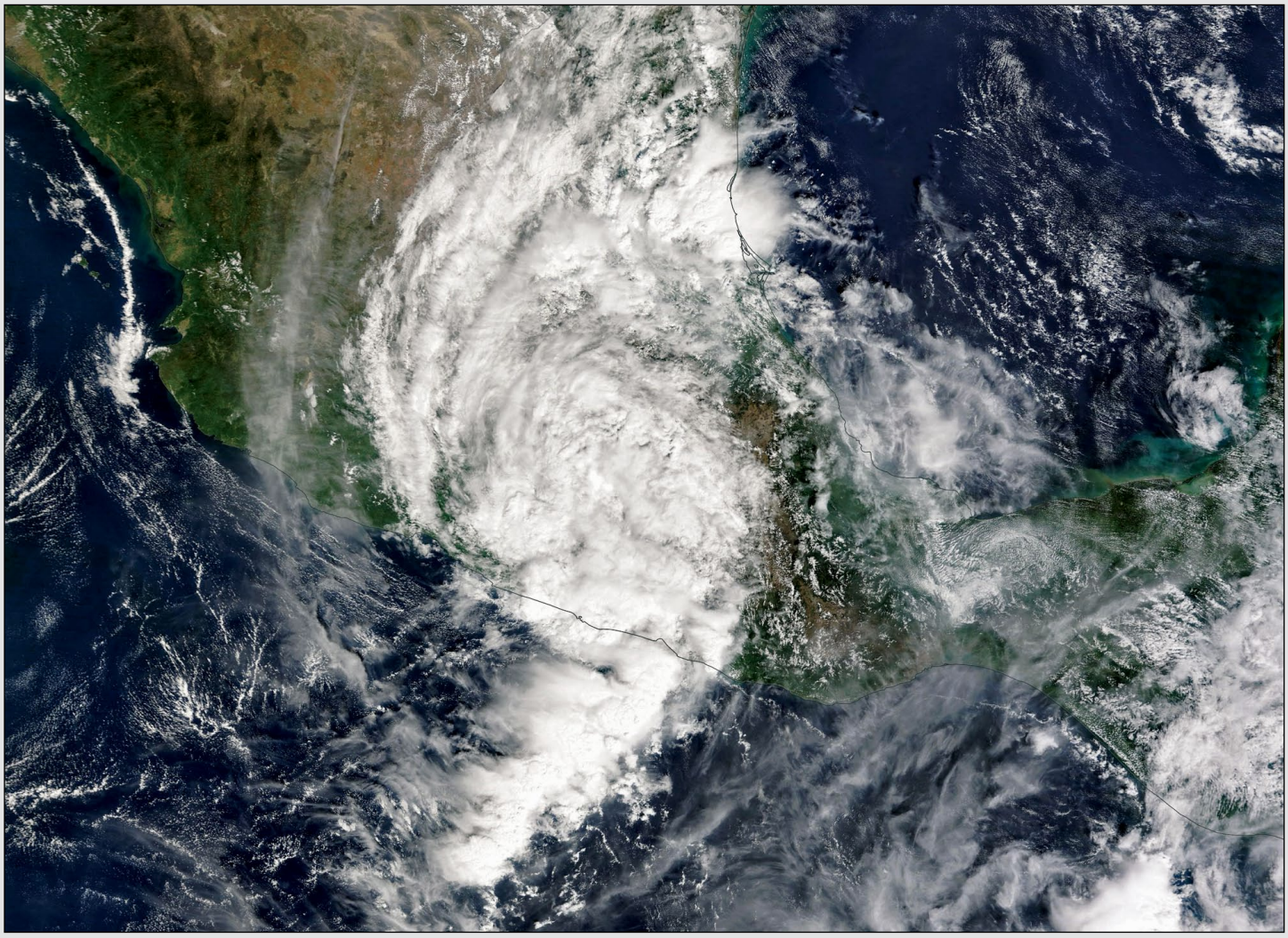

Image Credit: MODIS Land Rapid Response Team, NASA GSFC

Tropical Storm Otis first became a hurricane at 2:00 p.m. EDT on October 24, 2023, as it spun over the Pacific Ocean only 235 kilometres south-southeast of Acapulco, Mexico. At that time, its maximum sustained winds were 130 kilometres/hour. After a jaw-dropping rapid intensification, Otis became a catastrophic Category 5 storm with maximum sustained winds of 270 kph only ten hours later—and it was located only 70 km away from Acapulco. Hurricane Otis maintained this strength as it screamed ashore at 2:25 am EDT (1:25 local time) on October 25, becoming the strongest hurricane at landfall ever to strike Mexico's Pacific Coast.

Acapulco, a popular tourist destination and home to almost one million people, suffered severe damage. Social media posts—many using the terms 'destroyed' or 'ripped apart'— showed flooded streets, downed trees, and houses and hotels blown apart. CNN quoted Mexican President Andrés Manuel López as saying at a news conference:

"*In all of Acapulco there is not a standing [electric] pole". More than 500,000 homes and businesses lost power. In addition, 27 people have been confirmed to have died due to the hurricane and four remain missing*".

Once ashore, the fast-moving hurricane quickly weakened over inland mountains. At 5:00 pm EDT on October 25, the National Hurricane Center (NHC) issued its final bulletin on the storm as Otis had dissipated. At that time, the center of the remnants of Hurricane Otis were located about 260 km north-northwest of Acapulco and maximum sustained winds were 55 kph.

The Moderate Resolution Imaging Spectroradiometer (MODIS) on NASA's Terra satellite acquired the above true-colour image of the remnants of Hurricane Otis stretched over Mexico. Although winds were by then mild, the remnants nevertheless brought rain over a wide area.

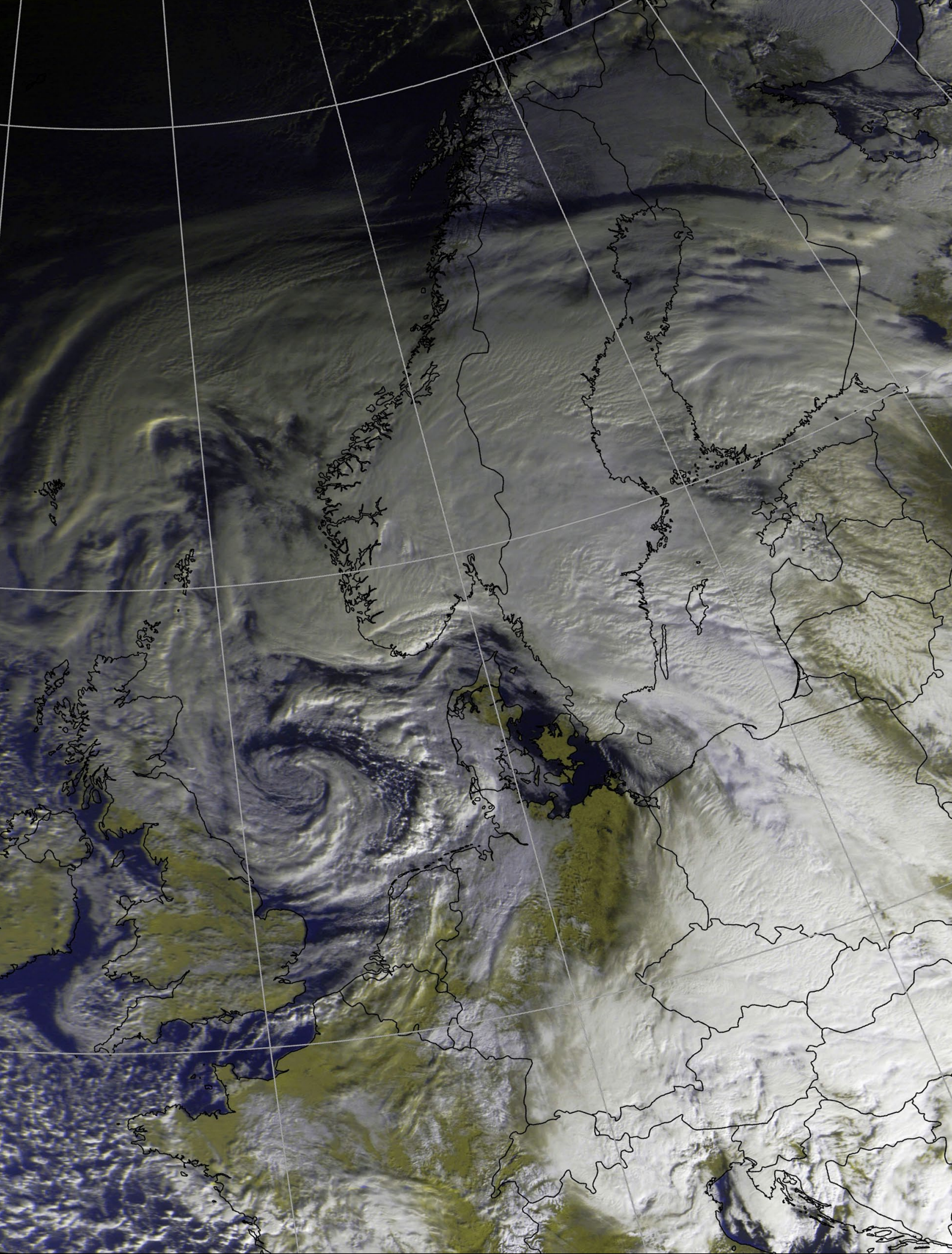

Joachim Scharrer acquired this Meteor M 2-3 image of **Storm Ciarán** over the North Sea on November 11, 2023 after it had lashed the British Isles with winds of up to 160 kilometres per hour, and caused extensive flooding, some places recording over a month's rainfall in just a few hours.

Sediments pour into the Adriatic Sea

Copernicus Image of the Day

Credit: European Union, Copernicus Sentinel-2 imagery

Torrential rain in early November 2023 caused severe flooding and widespread destruction throughout Italy. The increased surface runoff (i.e., the flow of water over the ground surface) eroded soils and filled rivers with sediment, which eventually washed all the way to the Adriatic Sea. The massive amount of sediment poured in the Adriatic Sea by the Angie and Po rivers shows clearly in this Copernicus Sentinel-2 image of the River Po delta, acquired on November 4.

The Copernicus Sentinel satellites provide valuable data to identify and delineate the extent of areas affected by such floods.

Floodwaters Fill Badwater Basin

NASA Eartg Observatory

Story by Lindsey Doermann

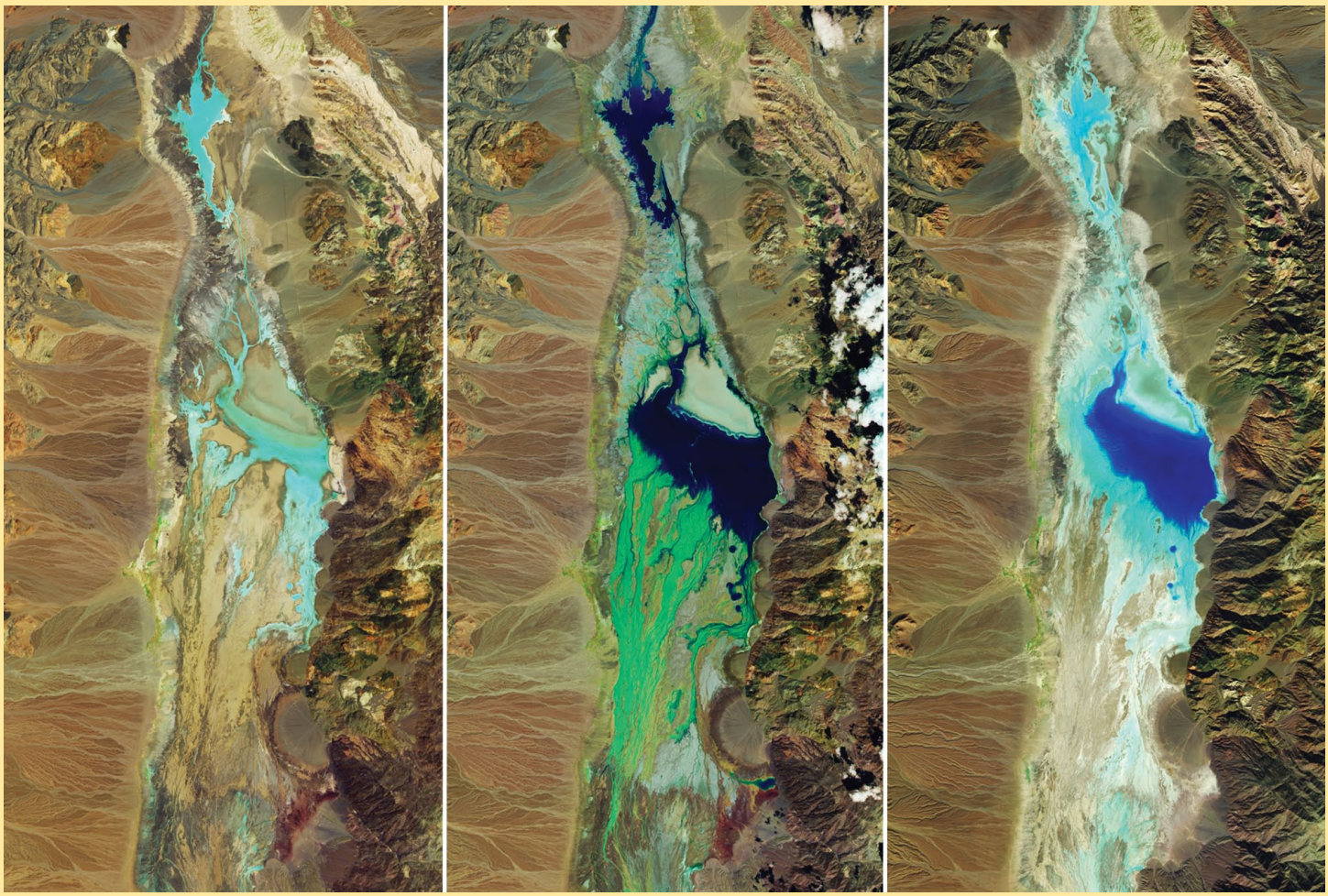

Three Landsat images of Death Valley's Badwater Basin

NASA Earth Observatory images by Wanmei Liang, using Landsat data from the U.S. Geological Survey

In August 2023, **Hurricane Hilary** made landfall in northern Mexico and soaked the Baja California peninsula, Southern California, and Nevada with rain. In **California's Death Valley**, flash floods damaged roads and other infrastructure, causing the national park to close for nearly two months. When visitors returned in mid-October, they witnessed an infrequent sight in this notoriously hot and dry place: a shallow ephemeral lake stretching for miles in Badwater Basin.

This series of images reveals hydrologic changes in the desert basin relative to August's heavy rain. The images are false colour to emphasize the presence of water, which appears in shades of blue. On July 5, 2023 (left), the basin contains relatively little moisture prior to flooding. In contrast, the August 22 image (middle) shows the aftermath of a record-setting rainy day. Both images were acquired by the OLI (Operational Land Imager) sensor on Landsat 8 using a band combination of 6-5-3.

On August 20, a weather station at Furnace Creek (north of this scene) recorded 56 millimetres of rain.

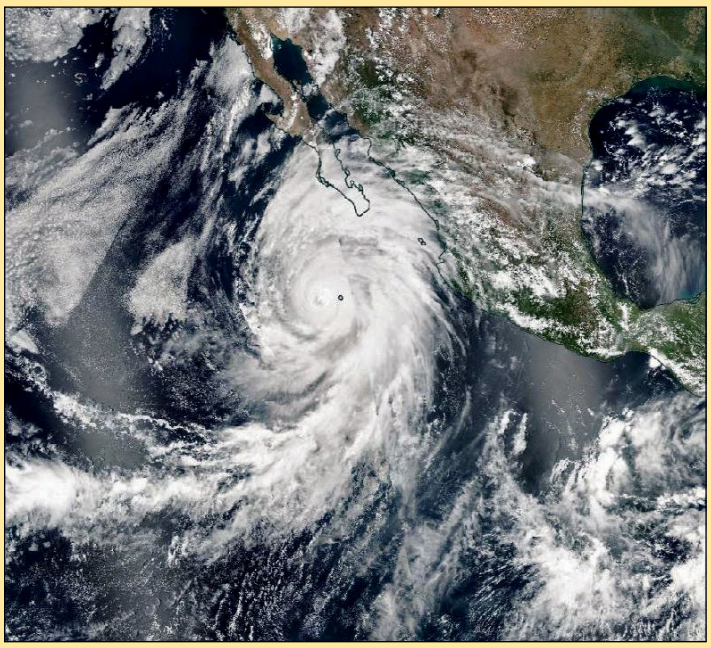

Hurricane Hilary imaged by the Suomi NPP satellite on August 18, 2023

Image: NASA Worldview Snapshots https://wvs.earthdata.nasa.gov/

The lake in Badwater Basin
Photo: K. Bott/NPS

This amount exceeds the area's average annual rainfall total of 55 millimetres, according to the National Park Service, and it breaks Death Valley's previous single-day rainfall record of 1.7 inches set in August 2022.

The image from November 2 (right), acquired by the OLI-2 on Landsat 9, shows the extent of water still present in the basin after more than two months. Around this time, national park officials stated that the lake measured approximately three by six kilometres, although it was only about five centimetres deep. Observers on the ground reported springs flowing, bighorn sheep feeding on new greenery, and even some wildflowers blooming—a rarity outside springtime.

Under more typical conditions, Badwater Basin is a vast and mostly dry salt flat—an expanse of approximately 520 square kilometres—surfaced with sodium chloride, calcite, gypsum, and borax. It is the lowest point in North America at 86 metres below sea level. The basin was once submerged by the much larger Lake Manly, one of several Great Basin lakes that existed during the cooler, wetter Pleistocene Epoch.

Today, it is uncommon but not unheard of for lakes to form in Badwater Basin. For example, storms and exceptionally rainy seasons filled in part of the basin in 2005, 2015, and 2019. There is no outflow from the basin, but the evaporation rate far outpaces the precipitation rate, rendering the lakes ephemeral. While park officials cannot be sure, they speculate that the current lake may dry up as soon as mid-November.

Retreat of the Upsala Glacier

Copernicus Image of the Day

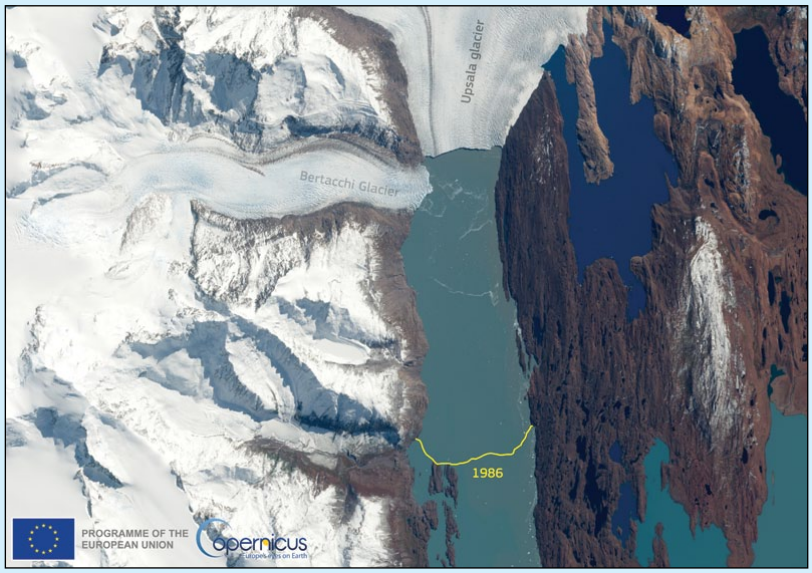

Credit: European Union, Copernicus Sentinel-2 imagery

The Upsala Glacier is ranked as the third largest glacier in the Southern Patagonian Ice Field. Unfortunately, many glaciers in the area, including Upsala, have significantly retreated over the last 50 years due to rising temperatures. The Upsala Glacier has been observed closely by Earth Observation satellites, which have shown that the glacier has retreated by around nine kilometres since 1986.

In this image, captured by one of Copernicus Sentinel-2 satellites on 22 September, the terminus of the glacier as it was in 1986 is highlighted with a yellow line. The retreat can clearly be seen as well as the fact that the Upsala and the Bertacchi Glaciers, which were still joined in 2016, are now separated.

Earth's Warmest October on Record

Copernicus Image of the Day

The Copernicus Climate Change Service (C3S) has recently released its latest monthly Climate Bulletin, which highlights that October 2023 was the warmest October on record globally. Notably, air temperatures exceeded those of the previous warmest October by a significant 0.85°C.

This data visualisation, based on C3S data, shows the surface air temperature anomaly for October 2023 across the European Continent. In that area, October 2023 was the fourth warmest October on record, 1.30°C higher than the 1991-2020 average, the warmest regions being Italy, the Balkans, and the central Mediterranean Sea.

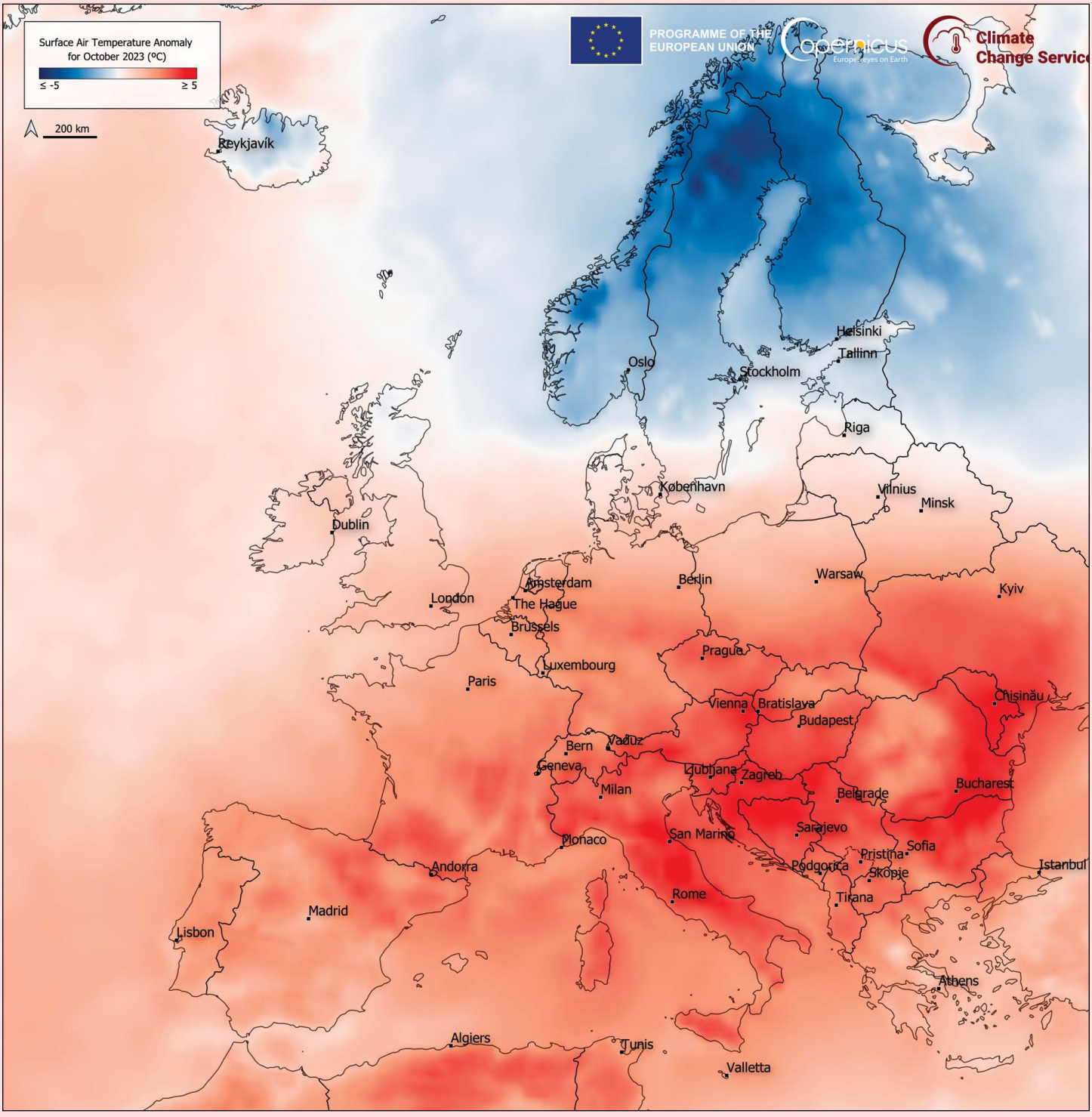

Credit: European Union, Copernicus Climate Change Service Data

Svalbard Satellite Station

An important part of the Copernicus Sentinel Ground Segment

Copernicus Image of the Day

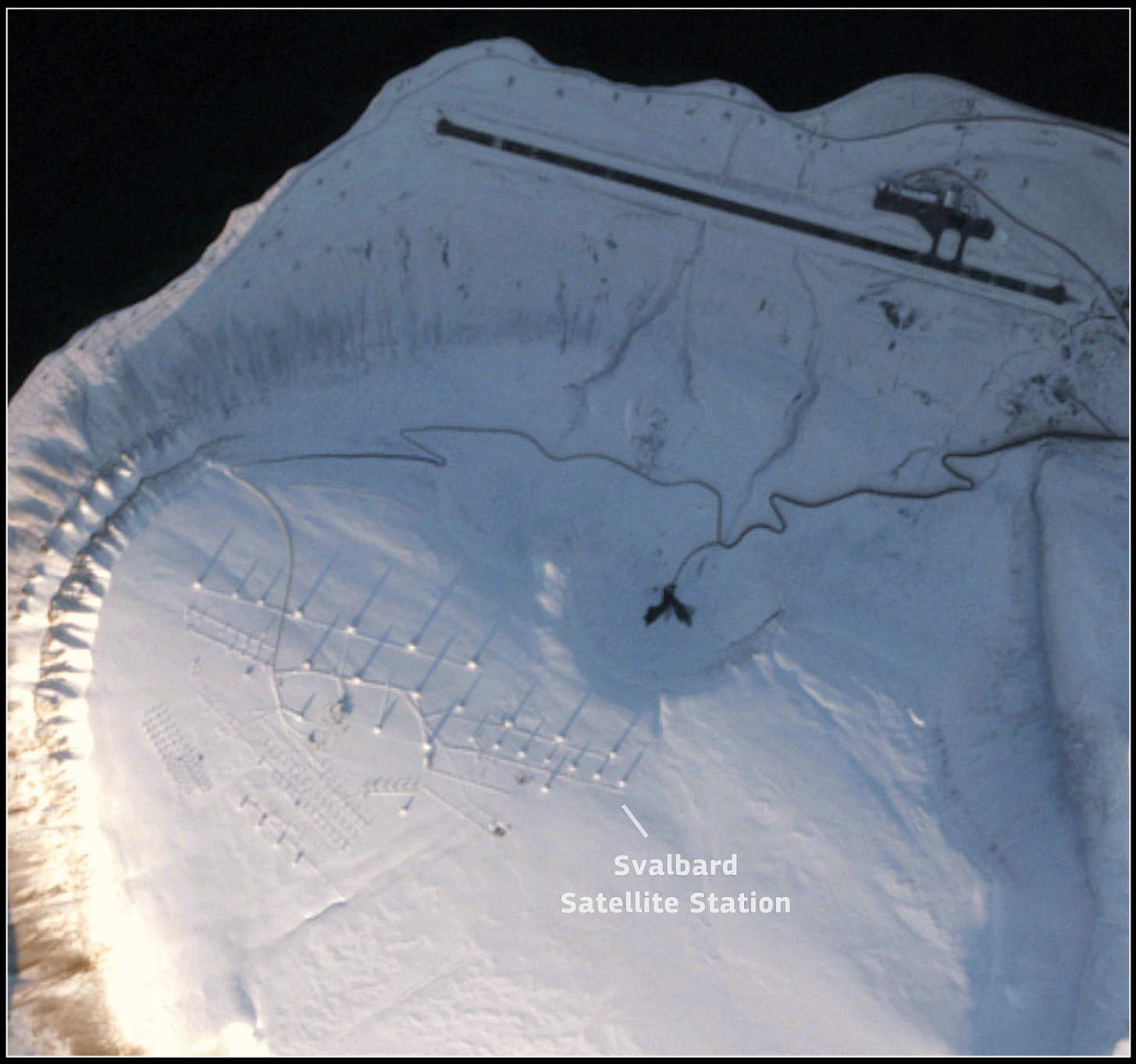

This image, acquired by one of Copernicus Sentinel-2 satellites on September 26, 2023, shows the **Svalbard Satellite Ground Station** (SvalSat), located on the island of Spitsbergen in the Norwegian archipelago of Svalbard.

The station is operated by Norwegian company *Kongsberg Satellite Services* and was inaugurated as part of the Copernicus Sentinel satellite ground segment in 2013.

Its location was selected because of its high latitude and proximity to the North Pole, and it is the only commercial ground station that can support polar-orbiting satellites every time they orbit the Earth (about 14 times a day).

The image shows the receiving antennas and their shadows projected on the snow.

Saharan Dust Plume Reaches Greek Coasts

Copernicus Image of the Day

This image showing a plume of Saharan dust reaching Greece was acquired by one of the Copernicus Sentinel-3 satellites on August 29, 2023. The large plume stretches hundreds of kilometres from the coast of Libya to the shores near the town of Pyrgos in Greece. These dust plumes have an impact on air quality.

The *Copernicus Atmospheric Monitoring Service* provides information and forecasts on the movement and distribution of these Saharan dust plumes, informing on air quality, their distribution and assisting local authorities in taking preventive measures to minimise their impact.

Credit: European Union, Copernicus Sentinel-3 imagery

Hurricane Nigel in the Atlantic Ocean

Copernicus Image of the Day

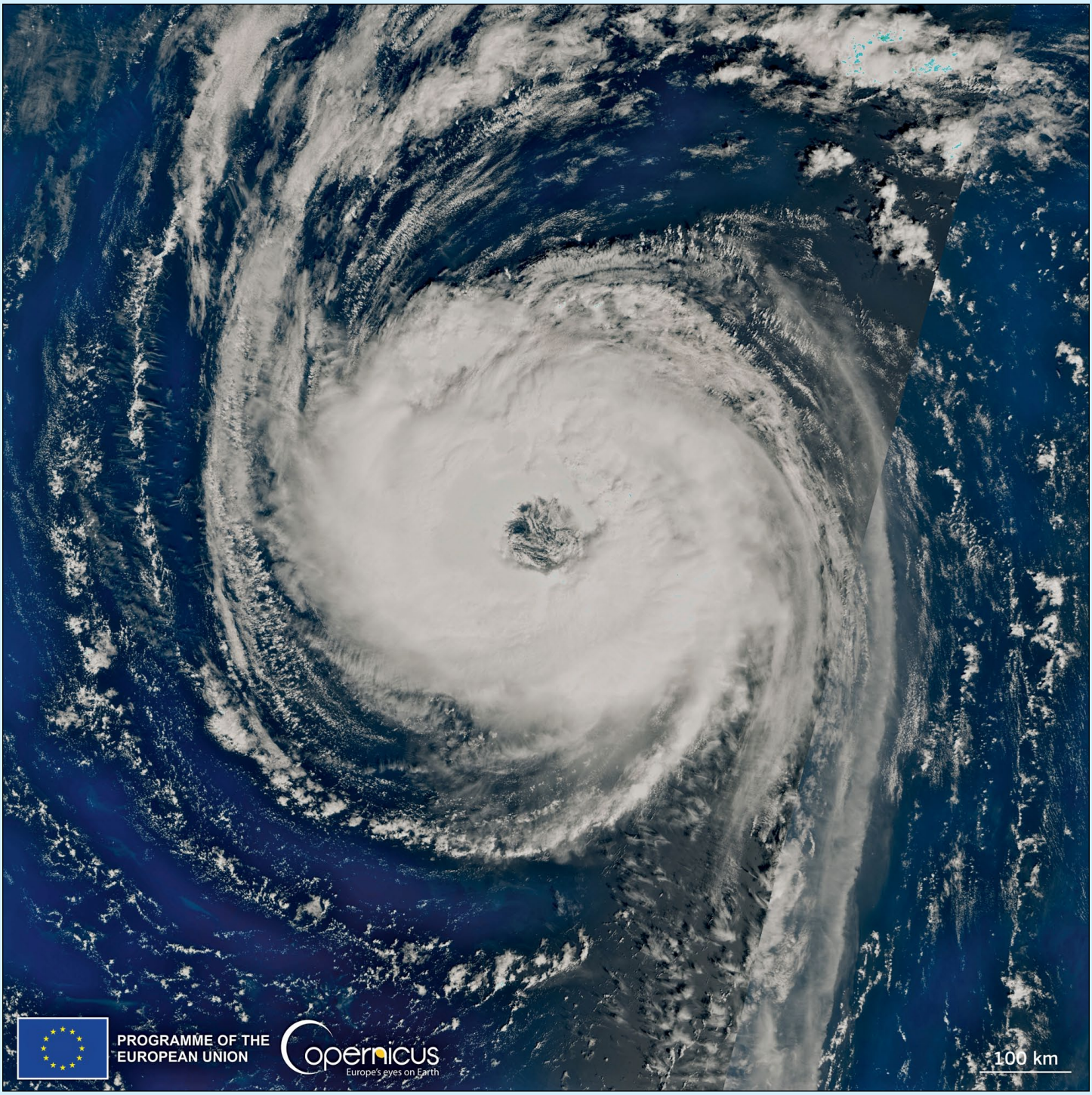

Credit: European Union, Copernicus Sentinel-3 imagery

This image, acquired on September 19, 2023 by one of the Copernicus Sentinel-3 satellites at 13:52:02 UTC, shows the beautifully proportioned Hurricane Nigel.

Nigel was the sixth storm of the Atlantic hurricane season. It formed on 16 September, and was situated approximately 1,000 kilometres southeast of Bermuda. Classified as a Category 1 hurricane, the US National Hurricane Center expected it to “rapidly intensify” to Category 3 over the following few hours. Nigel was not expected to make landfall, and no warnings were issued. However, its swells did lead to dangerous surf conditions near Bermuda.

Data derived from Copernicus Sentinel-3 satellites imagery bring improvements in the scientific understanding of the composition of the atmosphere and extreme weather events.

This impressive view including parts of the coastlines of British Columbia and Washington State, with Vancouver Island at centre, was acquired by John Jensen from a Meteor M 2-3 transmission on September 14, 2023

Elephant Island

European Space Agency

Image contains modified Copernicus Sentinel data (2023), processed by ESA, CC BY-SA 3.0 IGO

This rare, almost cloud-free view of the remote Elephant Island in Antarctica was captured in February 2023 by the Copernicus Sentinel-2 mission.

Lying in the Southern Ocean about 250 kilometres northeast of the tip of the Antarctic Peninsula, Elephant Island is one of the outermost of the **South Shetland Islands**. It owes its name to both the sighting of elephant seals along its shores and its elephant-like shape: in this image, the 'trunk' is partially covered by clouds.

This mountainous island is covered by ice. The highest peaks are Mount Pendragon, which reaches around 970 metres, visible on the southern end, and, moving northeast, Mount Elder, which reaches around 945 metres.

North of Mount Elder, the wide Endurance Glacier can be seen in the centre of the image. It is the main discharge glacier on the island and drains to the south and into the Weddel Sea. Thin sea ice, visible in light blue in front of the calving front, separates the glacier terminus from the open ocean waters.

The variations in the colour of the waters surrounding the island are due to sediment eroded by the flow of ice and carried by meltwater into the ocean. Small icebergs can be spotted, particularly off the western coast, as little white dots speckling the water. The white lines along the island coasts are the result of big waves crashing against the rocky steep cliffs.

Dramatic changes in Antarctica's ice have become synonymous with the climate crisis. The continued observations from satellites are key to surveying the remote polar regions. Satellites can monitor the melting ice sheets caused by rising temperatures and the subsequent rising of sea levels, as well as the impact on global ocean currents caused by the increased influx of freshwater into ocean. This is paramount to improving our understanding of the Earth system and to providing evidence on the impact of climate change.

You can explore the original much higher definition version of this image at:

https://www.esa.int/ESA_Multimedia/Images/2023/10/Earth_from_Space_Elephant_Island

A Veil of Haze over Northern Italy

Copernicus Image of the Day

Credit: European Union, Copernicus Sentinel-3 imagery

At the beginning of October, a high-pressure system brought clear skies to northern Italy, but also an increase in particulate matter concentrations in the Po Valley. According to local authorities, in cities like Milan and Turin, PM10 and PM2.5 levels were exceeding World Health Organisation thresholds and limits for key air pollutants that pose health risks.

Particulate matter (PM) describes constituents in the atmosphere which are not a gaseous, generally tiny particles of chemical compounds and other materials, some of which are toxic. Particles smaller than 2.5 micrometres in diameter are classified as PM2.5, while larger particles up to 10 micrometres in diameter are classified PM10. These tiny toxin particles can end up in the bloodstream and eventually lodge in vital organs such as the heart and brain.

Exposure to PM can result in serious health impacts, particularly in the young and the aged, as well as anyone suffering respiratory problems.

This image, acquired by one of Copernicus Sentinel-3 satellites on October 3, 2023, shows a veil of haze stretching from Piedmont to the Adriatic Sea.

Air quality monitoring and forecasting is one of the main focuses of the Copernicus Atmosphere Monitoring Service (CAMS).

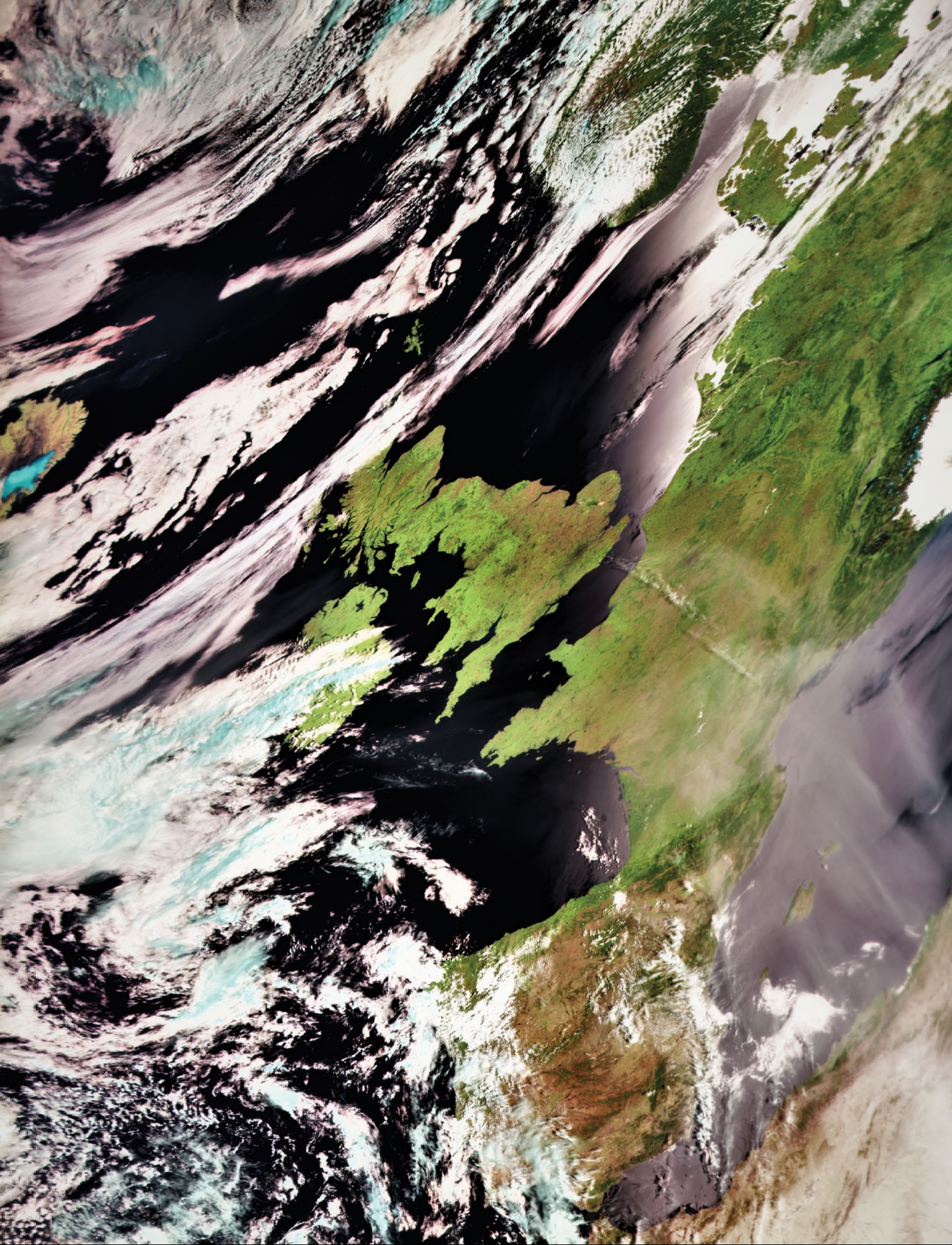

This unusual Meteor M2-3 HRPT image was acquired by Enrico Gobbetti on September 5, 2023 when the satellite briefly lost orientation

The Alps blanketed in white after the first Snowfall of the Year

Copernicus Image of the Day

Credit: European Union, Copernicus Sentinel-3 imagery

Following the autumn heatwave across Europe, the weather made a swift transition to winter on November 8 as the first snowfall of the season covered the Alps, the highest and most extensive mountain range in south-central Europe. Its peaks extend for 200 kilometres across Slovenia, Germany, Austria, Liechtenstein, Italy, Monaco, Switzerland, and France.

The Copernicus Land Monitoring Service product portfolio includes Snow & Ice (HR-S&I) Monitoring products, which provide high-resolution (20 m x 20 m) information derived from Copernicus satellites data on snow and ice conditions in the 38 Members States and Cooperating Countries of the European Environment Agency.

Third Eruption of 2023 at Mount Etna

Copernicus Image of the Day

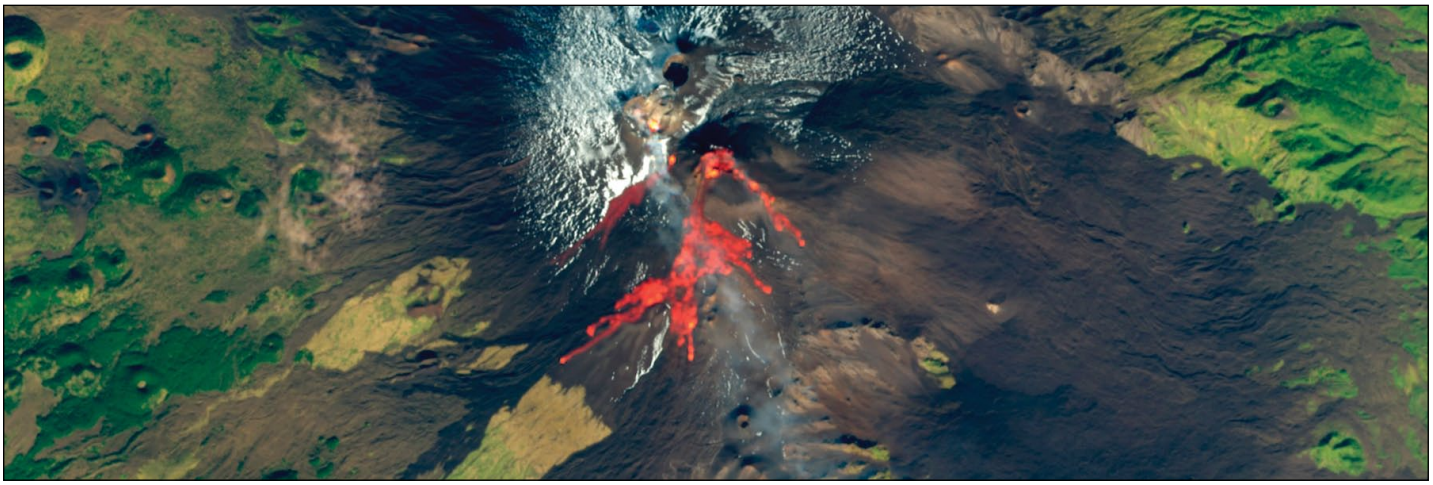

Credit: European Union, Copernicus Sentinel-2 imagery

Mount Etna erupted for the third time this year on November 12. The lava fountain activity lasted for several hours during the night, accompanied by a dense eruptive cloud laden with pyroclastic material (ash and lapilli) which fell in a narrow sector on the eastern slope of the volcano. The thermal signature of the cooling lava flow was still visible in this image acquired by one of the Copernicus Sentinel-2 satellites on November at 10:00 UTC. Copernicus Sentinel-2 satellites play an important role in monitoring volcanic activity thanks to their high spatial resolution and acquisition frequency.

Arctic Sea Ice falls to 6th Lowest on Record

NASA Earth Observatory

Story by Sally Younger (NASA's Earth Science News Team)

Arctic sea ice most likely reached its annual minimum extent on September 19, 2023, making it the sixth-lowest year in the satellite record, according to researchers at NASA and the *National Snow and Ice Data Center* (NSIDC).

Scientists track the seasonal and annual fluctuations because sea ice shapes Earth's polar ecosystems and plays a significant role in global climate. Researchers at NSIDC and NASA use satellites to measure sea ice as it melts and refreezes. They track sea ice extent, which is defined as the total area of the ocean in which the ice cover fraction is at least 15%. This map shows the sea ice extent on September 19, 2023.

Between March and September 2023, the ice cover in the Arctic shrank from a peak area of 14.62 million square kilometres to 4.23 million square kilometres. That's roughly 1.99 million square kilometres below the 1981-2010 average minimum of 6.22 million square kilometres. The quantity of sea ice lost was enough to cover the entire continental United States.

This year in the Arctic, scientists saw notably low levels of ice in the Northwest Passage.

> "*It is more open there than it used to be*," said Walt Meier, a sea ice scientist at NSIDC. "*There also seems to be a lot more loose, lower concentration ice—even toward the North Pole—and areas that used to be pretty compact, solid sheets of ice through the summer. That's been happening more frequently in recent years.*"

Meier said the changes are a fundamental, decades-long response to warming temperatures. Since the start of the satellite record for ice in 1979, sea ice has not only been declining in the Arctic, but also getting younger. Earlier starts to spring melting and ever-later starts to autumn freeze-up are leading to longer melting seasons.

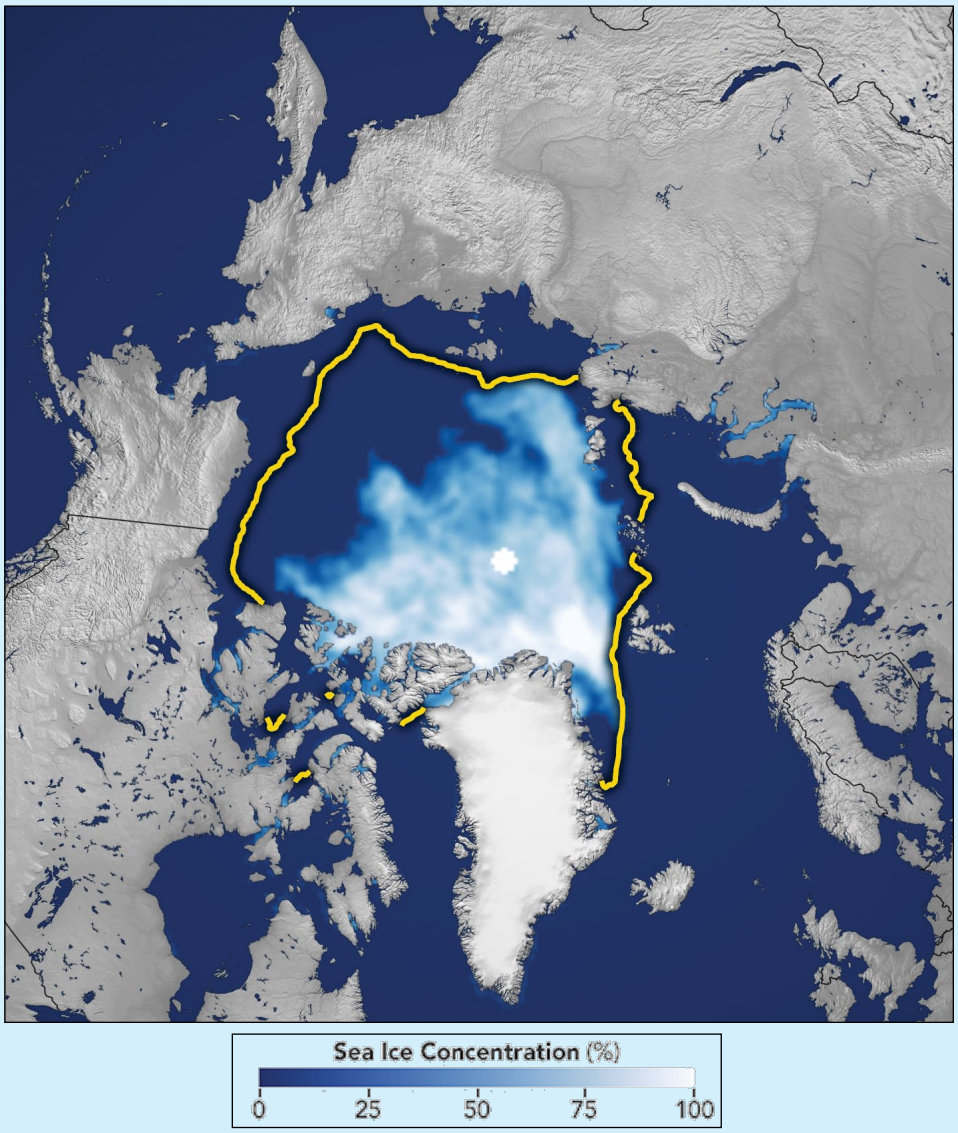

The yellow outline in this image shows the 1981-2010 median Arctic Ocean ice extent
NASA Earth Observatory image by Lauren Dauphin using data from the National Snow and Ice Data Center

Research has shown that, averaged across the entire Arctic Ocean, freeze-up is happening about a week later per decade, or one month later than in 1979.

Nathan Kurtz, lab chief of NASA's *Cryospheric Sciences Laboratory* at the agency's *Goddard Space Flight Center* in Greenbelt, Maryland, said that as the Arctic warms about four times faster than the rest of the planet, the ice is also growing thinner. Thickness at the end of the growth season largely determines the survivability of sea ice. New research is using satellites like NASA's ICESat-2 (Ice, Cloud and land Elevation Satellite-2) to monitor how thick the ice is year-round.

> Kurtz said that long-term measurements of sea ice are critical to studying what's happening in real time at the poles. "*At NASA we're interested in taking cutting-edge measurements, but we're also trying to connect them to the historical record to better understand what's driving some of these changes that we're seeing*."

Currently Active Satellites and Freqencies

Polar APT Satellites				
Satellite	**Frequency**	**Status**	**Format**	**Image Quality**
NOAA 15	137.6200 MHz	On	APT	Intermittent sync problem
NOAA 18	137.9125 MHz	On	APT	Good
NOAA 19	137.1000 MHz	On	APT	Good
Meteor M N2	137.1000 MHz	On	LRPT	Failed
Meteor M N2-3	137.9000 MHz	Off	LRPT	Variable [1]

Polar HRPT/AHRPT Satellites				
Satellite	**Frequency**	**Mode**	**Format**	**Image Quality**
NOAA 15	1702.5 MHz	Omni	HRPT	sync problem
NOAA 18	1707.0 MHz	RHCP	HRPT	Good
NOAA 19	1698.0 MHz	RHCP	HRPT	Good
Feng Yun 3C	1701.4 MHz	RHCP	AHRPT	Inactive [2]
Feng Yun 3D	7820.0 MHz	RHCP	AHRPT	Active {2}
Feng Yun 3E	7860.0 Mz	RHCP	AHRPT	Commissioning
Metop B	1701.3 MHz	RHCP	AHRPT	Good
Metop C	1701.3 MHz	RHCP	AHRPT	Good
Meteor M N2-2	1700.0 MHz	RHCP	AHRPT	Active [8]
Meteor M N2-3	1700.0 MHz	RHCP	AHRPT	Active

Geostationary Satellites				
Satellite	**Transmission Mode(s)**		**Position**	**Status**
Meteosat 9	HRIT (digital)		45.5°E	IODC - On
Meteosat 10	HRIT (digital)	LRIT (digital)	9.5 E	Off [4]
Meteosat 11	HRIT (digital)	LRIT (digital)	0°W	On [3]
GOES-13	GVAR 1685.7 MHz	LRIT 1691.0 MHz	61.6°W	[5]
GOES-14	GVAR 1685.7 MHz	LRIT 1691.0 MHz	105°W	Standby
GOES-15 (W)	GVAR 1685.7 MHz	LRIT 1691.0 MHz	128°W	On [6]
GOES-16 (E)	GRB 1686.6 MHz	HRIT 1694.1 MHz	75.2°W	On [7]
GOES-17	GRB 1686.6 MHz	HRIT 1694.1 MHz	137.3°W	On [7]
GOES 18	GRB 1686.6 MHz	HRIT 1694.1 MHz	137.0°W	On [7]
Himawari-8	No direct download	Data is only available via the HimawariCast service	140.7°E	Onw
Himawari-9	No direct download		1450.7°E	On
Feng Yun 2E	SVISSR (digital)	LRIT (digital)	86.5°E	On
Feng Yun 2F	SVISSR (digital)	LRIT (digital)	112.5°E	Standby
Feng Yun 2G	SVISSR (digital)	LRIT (digital)	99.5°E	On
Feng Yun 2H	SVISSR (digital)	LRIT (digital)	79.0°E	On
Feng Yun 4A	HRIT (digital)	LRIT (digital)	99.5°E	On
Feng Yun 4B	HRIT (digital)	LRIT (digital)	Just	Launched

Notes

1 Currently under commissioning, M2-3 regularly swaps both frequency between 137.1 MHz and 137.9 MHz. There are also regular switches in Symbol Rate between 72,000 and 80,000.
2 These satellites employ a non-standard AHRPT format and cannot be received with conventional receiving equipment.
3 Meteosat prime Full Earth Scan (FES) satellite
4 Meteosat prime Rapid Scanning Service (RSS) satellite.
5 Repurposed by US Space Force
6 GOES 15 also transmits EMWIN on 1692.700 MHz GOES 16 also transmits EMWIN on 1694.100 MHz GOES 17 also transmits EMWIN
7 GOES Rebroadcast (GRB) provides the primary relay of full resolution, calibrated, near-real-time direct broadcast space relay of Level Ib data from each instrument and Level 2 data from the Geostationary Lightning Mapper (GLM). GRB replaces the GOES VARiable (GVAR) service.
8 Following a collision with a micrometeorite, the power system aboard Meteor M2-2 has been compromised. AHRPT is still being transmitted when the solar panels are sunlit, but there is insufficient battery power to enable the LRPT stream.
9 Japanese satellits MTSAT-1R (Himawari-6) and MTSAT-2 (Himawari-7) are no longer active and are probably retired. Current Japanese operational geostationary satellites are Himawari-8 and Himawari-9).